

## Catalan, Motzkin, and Riordan numbers

Frank R. Bernhart

140 Whiteford Road, Rochester, NY 14620-4640, USA

Received 27 March 1997; revised 30 December 1998; accepted 15 January 1999

Dedicated to H.W. Gould, on the occasion of his seventieth birthday

---

### Abstract

Catalan numbers  $C_n$  are widely known and studied and more recently the Motzkin numbers  $M_n$  have been celebrated. Closely joined to the Motzkin sequence is a sequence of unnamed numbers  $\gamma_n$ , also growing in importance. Here they are denoted by  $R_n$ , where  $R$  stands for Riordan. In 1977, using the planar coloring schemes defined by W. T. Tutte, I discovered that these numbers answer an old problem about linearly independent chromatic polynomials.

Planar coloring schemes for an  $n$ -ring can be viewed as the subset of cyclically spaced non-crossing partitions of an  $n$ -cycle, and they define a natural geometric basis for chromatic polynomials on the  $n$ -ring.

This article presents a unified overview of Catalan, Motzkin, and  $R$ -numbers, intended as a primer of sequences and techniques, combinatorial structure and recursion, generating function equations, difference triangles, and Lagrange inversion. Direct combinatorial correspondences are highlighted. © 1999 Published by Elsevier Science B.V. All rights reserved.

---

### 1. Introduction and overview

Catalan numbers  $C_n$  have been widely encountered and widely investigated. The research bibliography of Gould [22] contains a wealth of references. The Motzkin numbers  $M_n$  have more recently been emphasized by Donaghey and Shapiro [20]. Their work shows the useful close connection between  $C_n$  and  $M_n$ , as well as exhibiting fourteen varied counting problems which lead to the Motzkin numbers.

Closely joined to the Motzkin sequence is a sequence of unnamed numbers  $\gamma_n$ . Apparently Riordan was the first to emphasize the relationship and derive crucial formulas [31]. There is no hint in either of the papers [20,31] that the companion numbers  $\gamma_n$  were fated to appear in quantum chemistry [2], Hilbert spaces [1], and other areas [25].

In this paper these numbers are denoted by  $R_n$  and called *Riordan numbers* (alternately *ring numbers*). The connection with rings is as follows. In 1977 I rediscovered

---

*E-mail address:* frb6006@cs.rit.edu. (F.R. Bernhart)

these numbers in the context of the chromatic theory of planar maps and graphs. *Planar coloring schemes* had recently been defined by W. T. Tutte (see [45]) as a result of his reflections on the seminal paper of Birkhoff and Lewis [10]. In particular, he was seeking a better foundation for the mysterious identities holding among what Birkhoff and Lewis called ‘constrained chromatic polynomials’. For an introduction to the theory of chromatic polynomials, see [8,29,30,43,44].

Planar coloring schemes for an  $n$ -ring can be reinterpreted as *cyclically spaced non-crossing partitions* of an  $n$ -cycle. This subset of the noncrossing partitions is presented below as the combinatorial family [R2] of Section 3.2.

The  $n$ -cycle corresponds to the older concept of a ‘ring’ of regions in a planar map. The ring of order  $n$  has been fundamental to the study of the Four Color Conjecture ever since Birkhoff’s pioneering paper in 1913 [9]. The family [R2] turns out to be a natural geometric basis for chromatic polynomials on the  $n$ -ring. Consequently, the number  $R_n$  is the number of linearly independent chromatic polynomials when the  $n$ -ring contains an arbitrary configuration.

At the time I was not yet aware of the close kinship between  $R_n$  and  $M_n$  or the equation  $M_n = R_n + R_{n+1}$ . In Sloane’s remarkable Handbook of Integer Sequences [41], the Motzkin number sequence is listed as #456, the Catalan sequence is listed as #577, and the  $R$ -sequence is not listed (it should follow #1023). I am indebted to personal correspondence with D.G. Rogers for putting me on the right track not long after.

The purpose of this article is to present a unified overview of the Catalan, Motzkin, and  $R$ -number sequences and to show that  $R$ -numbers are equally as fundamental as the Motzkin numbers. Certain other sequences also make an appearance. The following table displays the beginnings of these sequences and certain related sequences that will also be considered. The identification number  $Mnnnn$  comes from the Encyclopedia of Integer Sequences [42], the worthy successor of Sloane’s Handbook.

Table of sequences

$n$		0	1	2	3	4	5	6	7	8	9	10
M1459	$C_n$	1	1	2	5	14	42	132	429	1430	4862	16796
M2587	$R_n$	1	0	1	1	3	6	15	36	91	232	603
M1184	$M_n$	1	1	2	4	9	21	51	127	323	835	2188
M1484	$B_n$	1	1	2	5	15	52	203	877	4140	21147	115975
M3423	$V_n$	1	0	1	1	4	11	41	162	715	3425	17722
M3400	$A_n$	1	0	1	1	4	10	34	112	398	1443	5387

In Section 3 below, three sample counting problems are given for each of the sequences  $C_n$ ,  $R_n$ , and  $M_n$ . The problems are related to points on a circle or to sets of plane trees. The description of these classes is deliberately kept somewhat informal, but not, we hope, at the cost of clarity.

The discussion centers first on combinatorial structure and recursion. Wherever feasible, direct combinatorial correspondences are used. With the exception of a few of the more striking correspondences, I have not tried to locate in the literature the very first use of each. Some of them have been discovered and rediscovered many

times. Here the intention has been to present each correspondence in visually convincing form, suppressing tedious details. A number of correspondences in one form or another are found in the papers of Rogers [32–35].

A sample of lattice path families and families of increasing bipartite graphs (as in [20]) are grouped in one section. The methods and transformations suggested there can be used to produce an almost unending spate of such families.

The next section uses difference triangles and related patterns as an easy bridge to certain connection formulas — proofs in the literature tend to be longer and less appealing. This is followed by a brief introduction to solution of functional equations by Lagrange inversion.

In the last section, the tie between  $R_n$  and chromatic polynomials is described in greater detail. It is hoped that this presentation can be useful as a primer of sequences and techniques.

## 2. Useful definitions

A *partition* of an  $n$ -set is a division of a set of  $n$  elements into classes (called also blocks), where each element is assigned to exactly one class. Here the elements will be vertices on a circle. It is convenient to assume that the vertices are evenly spaced and numbered  $1, 2, \dots, n$  in counterclockwise order, starting with 1 at the bottom of the circumference. When the labeling is implicitly understood, rotating the diagram counterclockwise by  $360/n$  degrees in effect advances the number labels  $k$  to  $k+1 \pmod{n}$ . Similarly, the diagram may be reflected in a vertical line. In constructing long tables of diagrams it is efficient to list only diagrams that are not equivalent by rotation or reflection.

The *graph of the partition* is formed by joining cyclically the vertices of each class with edges, namely chords of the circle. (In some of the diagrams, we will take the liberty of curving edges between nonconsecutive vertices, simply as a visual aid.) This is usually called the *circular representation* of the partition. Singleton classes are isolated vertices. Doubleton classes are a pair of vertices joined by one edge. If the maximum vertex degree in the graph is one, then every class is a singleton or doubleton.

The partition is *noncrossing (planar)* in case the edges do not cross. It is *cyclically spaced (or feasible)* in case adjacent vertices are never joined by an edge, and *infeasible* otherwise. See Fig. 1 (note curving in the middle diagram). The circles here are not officially part of the graph.

A useful notation for partitions is to employ the same letter (or number) symbol for all vertices in the same class. The partition is displayed as a letter sequence. This representation is the *scheme* of the partition. The scheme is *orthodox* if it lexicographically first among all schemes for a given partition, i.e. *bab*c is not orthodox, but is equivalent to a unique orthodox scheme, namely *ab*ac. When the partition happens to be feasible, the associated schemes are just colorings in the usual sense of a (cyclically) labeled circuit.

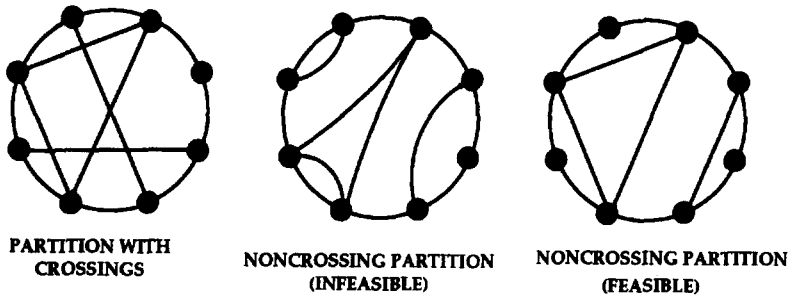
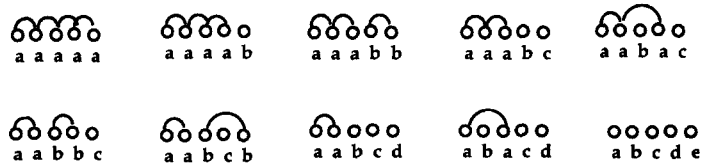


Fig. 1.



**BASIC NONCROSSING 5-POINT PARTITIONS:  
Row Diagrams & Equivalent Codes**

(A) (Rotate to get ALL 42 NC Partitions)



**BASIC PARTITIONS WITH CROSSINGS**

(Rotate to get All Ten)



(B)

Fig. 2.

Adopting this convention, we find all partitions for  $n = 5$ . There are 42 noncrossing partitions, found by *rotating* the ten examples of Fig. 2A (thus *aaabc* rotates to *aabca*, etc). The rotational classes have size 1, 5, 5, ..., 5, 1. There are ten partitions with crossings, found as rotations of the two shown in Fig. 2B. There are exactly eleven of the 42 partitions which are feasible, and five of them are noncrossing. From here on the abbreviation NC will be used for ‘noncrossing’.

A row diagram is constructed on top of each sequence using arcs which are tops of circles. A row diagram is usually called the *linear representation* of the NC partition.

The graph of a NC partition may be generalized in a useful way. Suppose that vertices placed on a circle are joined two at a time in any fashion by NC chord-edges (Fig. 3, first diagram). The result happens to be a (vertex) labeled outerplane graph, but several warnings are needed. An abstract graph can be labeled in various ways. For any given labeling, the vertices may be arranged on a circle in the indicated order, and the edges represented by chords. If at least once the chords do not cross, the graph is outerplanar. However, not all labelings give an outerplane form. Considering only

SMALL NUMBERS:  $(n)$  COUNTS THE VARIANTS OBTAINED BY ROTATION  
 $(n+n)$  COUNTS VARIANTS FOR DIAGRAM & MIRROR IMAGE

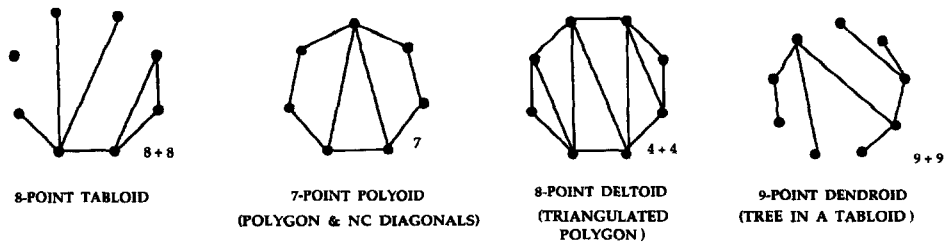


Fig. 3.

those which do, different labelings sometimes give the same outerplane embedding, and sometimes not.

Our kind of labeled embedding is related to the concept of a book embedding, as given by Bernhart and Kainen [6]. Book embeddings have proved helpful in computer applications [13]. A graph which is embedded in a 1-page book is essentially the type of labeled graph considered above, with vertices on a circle (or line) and edges as straight segments (or arcs in a half-plane). It will be called a *tabloid* in this article as well as others in preparation [7] (the name suggests both a table and lack of depth). An alternate name is ‘ladder graph’ [17], but that term is less appropriate, and indeed was already in use (see [30] for instance).

Several tabloid subclasses are noteworthy. The *polyoid* (called also *dissection*) is a regular (or just convex) polygon, with optional NC diagonals. Edges of the polygon are *outer* edges; diagonals are *inner* edges. By deleting selected outer edges, arbitrary tabloids are obtained from polyoids. Counting polyoids is an old problem going back to Kirkman and Cayley in the nineteenth century (see Brown [11] for a discussion of the history). A further subclass is the polyoids to which no inner edges can be added, which is just the dissection of polygons into triangles. These will be known as *deltoids*. Trees in tabloid form will be called *dendroids*. Examples of these classes are in Fig. 3.

### 3. Numbers that often recur

#### 3.1. Recurring numbers: Catalan

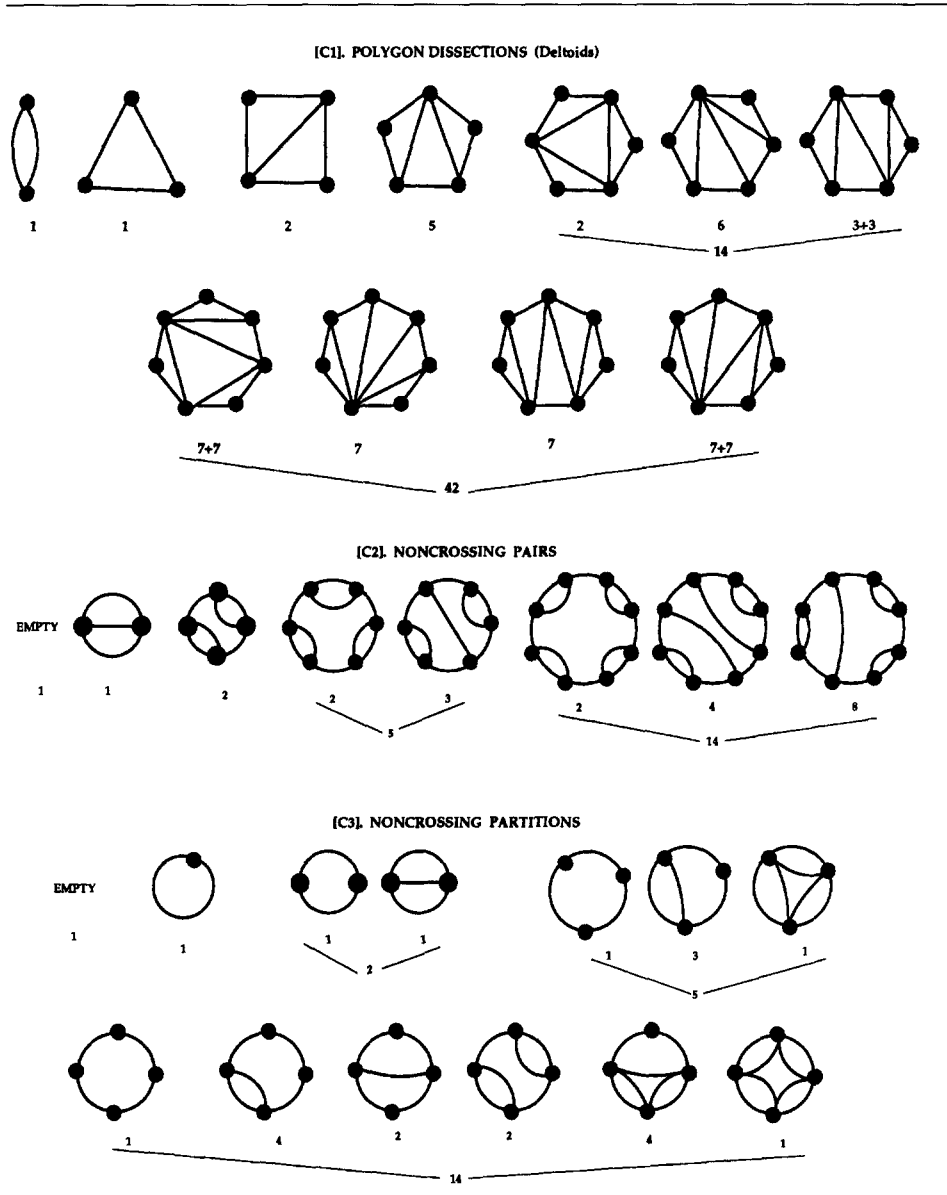
The Catalan numbers  $C_n = \frac{1}{n+1} \binom{2n}{n}$  come up in a large number of counting problems. Table 1 shows three families of Catalan type: a family of deltoids, and two families of NC partitions. They are described as follows.

[C1] *Triangulations of a polygon, or deltoids*

The family of complete dissections of a convex  $(n+2)$ -gon.

Probably the most widely familiar example, deltoids (our term) can be defined by putting  $n+2$  points on a circle and joining as many pairs as possible with NC diagonals.

Table 1  
Catalan families (Summary of rotation/reflection variations)



There will always be  $n + 2$  polygonal or outer edges and  $n - 1$  inner diagonals making  $2n + 1$  edges and  $n$  triangles. By convention, the smallest case is  $n = 0$  or a digon. Deltoids are a subclass of polyoids.

[C2] *Planar pairs* (noticed by Errera [21])

Place  $2n$  points on a circle, then join them pairwise with  $n$  NC chords.

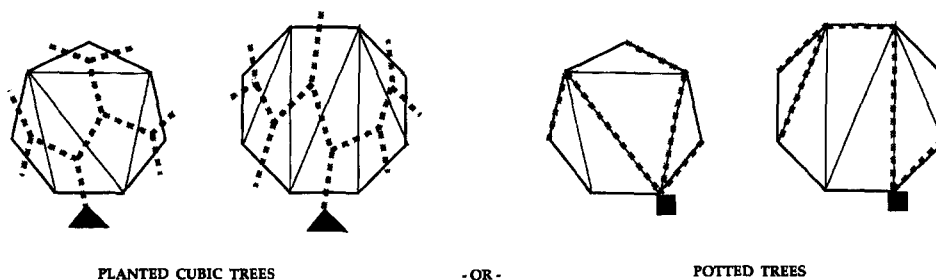


Fig. 4.

This family, delightfully elementary, is essentially the family of NC partitions of an even number of points, consisting entirely of doubletons (the graph has valency exactly one). We include the case  $n = 0$  with count equal to one.

[C3] *Noncrossing partitions*

Place  $n$  points on a circle and partition them into disjoint classes that do not cross. The noncrossing requirement was defined in the last section.

The family C1 can be dualized. Put  $n + 2$  new points on the circle, as midpoints of the arcs defined by the original set. The new points can be moved away from the center of the circle for greater clarity. Also put one point inside each of the  $n$  triangles. To obtain the dual figure, join with an edge (called dual edge) the two points on either side of each original edge. The result is a ‘cubic’ or trivalent planar tree planted in the plane. All of the endpoints of the tree lie on the circle; the root is the endpoint in the first arc, marked with a triangle (Fig. 4).

The stalk is the edge attached to the root vertex. Suppose the stalk of any planted plane tree (not necessarily cubic) is shrunk to a point. The result of shrinking the stalk is a potted plane tree. A small box marks the root. The root vertex of a potted tree will often have degree greater than one, but not always.

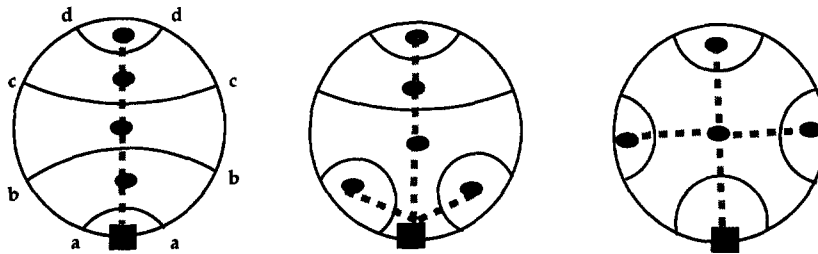
The right half of Fig. 4 show how a potted tree can be excavated from a deltoid: the ‘right’ side of every triangle is shaded. If the reader does not see how to distinguish ‘base’ edge, ‘left’ edge, and ‘right’ edge for each triangle, then look at the left two diagrams of Fig. 4. Moving away from the root of the planted cubic tree, at each fork (i.e. cubic vertex) the rightmost option continues with an edge which exits the triangle via its ‘right’ side.

We illustrate in Fig. 5 the dual tree of a planar pairing [C2]. There is one vertex for each region and one dual edge for each inner edge. Equivalent row diagrams and schemes are shown. Moreover, each letter pair can be changed to a parenthesis pair: ‘(,)’.

The cubic trees dual to the family [C1] and the plane trees dual to the family [C2] are related by a simple correspondence that has one arbitrary choice between right and left. We have already seen this implicitly in Fig. 4. An explicit version is now described (see Fig. 6).

Start with a planted cubic tree. The terms ‘fork’, ‘right’ edge, and ‘left’ edge are the same as above. Identify or mark the rightmost edge at each fork and include the

NC PAIRS & POTTED TREES AS "DUALS"



EASILY OBTAINED EQUIVALENT REPRESENTATIONS

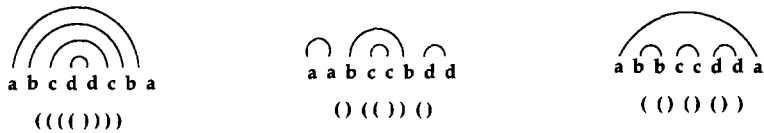


Fig. 5.

Arbitrary Plane Tree  $\alpha$   
Has Left Cubic Associate  $\lambda$  and Right Cubic Associate  $\rho$

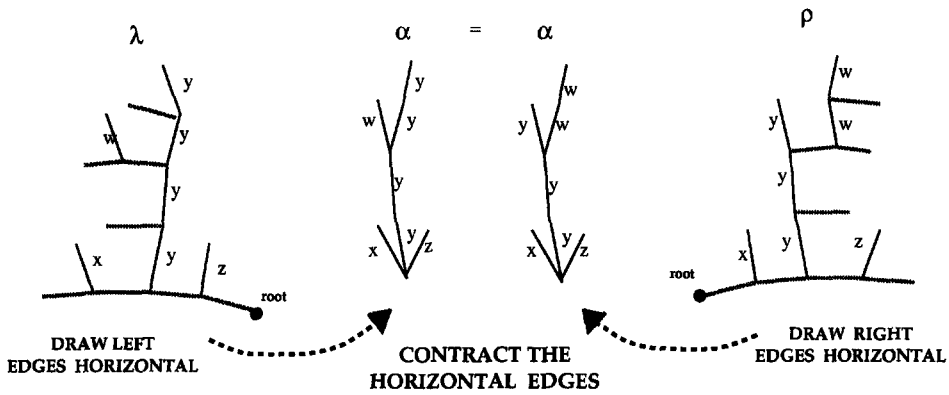


Fig. 6.

single edge at the root. Then shrink or contract these edges to get a new tree. The transformation is written  $\lambda \rightarrow \alpha$  if leftmost edges are contracted and  $\rho \rightarrow \alpha$  if rightmost edges are contracted. This is visually more striking if the marked edges are first drawn horizontally and thickened, as in the figure. The unmarked edges are almost vertical, so that the tree  $\alpha$  is plainly seen to be constituted from the upward paths marked  $x, y, z, w, \dots$  in the figure. The schema here is a modification of the one found in [15] (Fig. 6).

Since the tree  $\alpha$  does not have mirror symmetry (vertical axis) the associated trees  $\lambda$  and  $\rho$  are not a mirror pair.



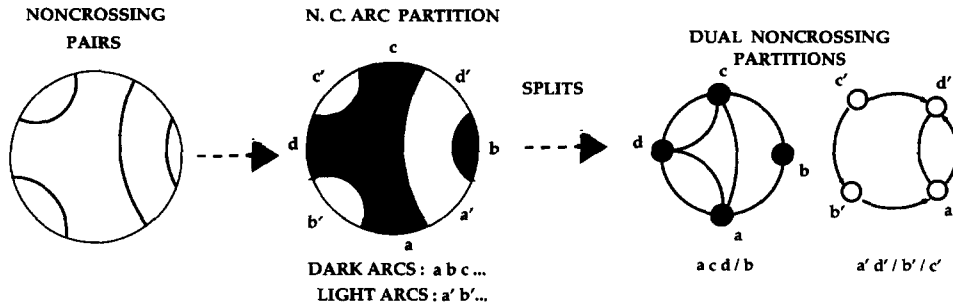


Fig. 7.

If we reverse the  $\lambda$  transformation and combine it with the  $\rho$  transformation, we get  $\rho \rightarrow \alpha \rightarrow \lambda$  which is an automorphism on the class of planted cubic trees. Donaghey [19] and Kettle [26] have considered in detail the structure of this automorphism.

Alternately, we can combine in the other order. Let tree  $\lambda$  be redrawn in the  $\rho$  form to get  $\lambda = \rho'$ . Then an automorphism  $\alpha \rightarrow \lambda = \rho' \rightarrow \alpha'$  on the set of all plane trees is created.

Consider now how to find a correspondence between [C2] and [C3]. Take a member of [C2] and place  $2n$  new points in the  $2n$  arcs. Inside the circle, the  $n$  chords divide the circle into  $n+1$  regions. The boundaries induce in a natural way an NC partition of the new points. By shading the regions dark/light as shown in Fig. 7 (in checkerboard fashion), we see that each (bent) chord separates dark from light, and hence the new points fall alternately into one of two classes; also the NC partition divides naturally into subpartitions. Moreover, the ‘dark’ partition and the ‘light’ partition determine each other, and determine the NC pairing (leftmost diagram). Thus, we have obtained two correspondences between [C2] and [C3], and a ‘duality’ within [C3] to boot.

More precisely, we follow the lead of Simion and Ullman [39] by using the labels  $abc \dots$  counterclockwise, alternating with  $a'b'c' \dots$  going clockwise. The first vertex 1 from the  $2n$  vertices of the NC pairing must fall between  $a$  and  $a'$ , with order  $a, 1, a'$  (counterclockwise). The details of the construction of a partition of  $a'b'c' \dots$  from a partition of  $abc \dots$  will be omitted.

This plan ensures that the dual of the dual is the original (we have an involution). Moreover, it is not hard to show that for  $n = 2m$  there are no self-dual partitions, and for  $n = 2m + 1$  there are  $C_m$  self-dual partitions. A beautiful corollary follows: the only odd Catalan numbers are the  $C_n$  with  $n = 2^k - 1$ .

The standard recursion for Catalan numbers is

$$C_{n+1} = C_0 C_n + C_1 C_{n-1} + \dots + C_n C_0.$$

This recursion is easy to establish in terms of recursive structure in the families [C1], [C2], [C3]. The idea is to decompose a member of the order  $n+1$  family by a reversible method into two smaller examples, with orders  $i, j$  and  $i + j = n$ .

In [C1] removing the ‘base’ edge  $12$  decomposes the figure. In [C2] consider the division of the circle produced by the edge from vertex  $v_1$  (see Fig. 8).

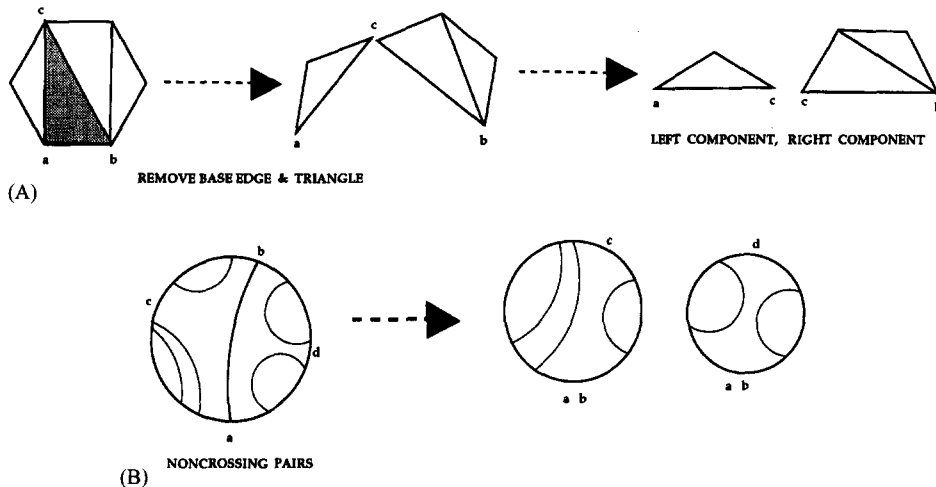


Fig. 8.

A similar decomposition for family [C3] is an elementary simplification of a Motzkin decomposition given later. It is discerned by focusing on the right-hand side of Fig. 13B. The details are left to the reader.

Whenever a decomposition is given for one family, it can be transferred to any other family that has an explicit correspondence to the given one. The more natural the correspondence, the easier it is to make the transfer.

The standard recursion for  $C_n$  is concisely captured by the equation

$$y = 1 + xy^2,$$

where  $y = \sum_{n=0}^{\infty} C_n x^n$ . This ‘characteristic’ equation determines  $y$  uniquely as a power series in  $x$  with constant term 1. The recursive procedure for calculating the coefficients is exactly the standard Catalan recurrence, and so the power series is the ‘enumerator’ or generating function (g.f.) for the Catalan sequence.

There are many ways to derive simpler recursions and exact formulas for Catalan numbers. See for example [40].

Now return to the three examples of Fig. 5, where scheme  $abcd d c b a$  may be reinterpreted as matched pairs of parentheses  $((((( )))$ ). The scheme also may be diagrammed as the outline of a mountain range (or Dyck path). Scan the scheme from left to right. The first letter of a pair dictates a step up (a move from  $(x, y)$  to  $(x+1, y+1)$ ), and the second member of the pair dictates a step down (a move from  $(x, y)$  to  $(x+1, y-1)$ ). The mountain range sits on the  $X$ -axis, starts at the origin, and ends at  $(2n, 0)$  without dropping below the axis. It can be reordinatized to be a lattice path of  $2n$  steps joining the origin to  $(n, n)$  which does not go below the diagonal  $x = y$ .

Put a chess king in the upper left corner of a chessboard, and let the board have infinitely many rows numbered  $0, 1, 2, 3, \dots$ , and the same with columns. The squares below the downward diagonal are forbidden, and the king moves only to the right or

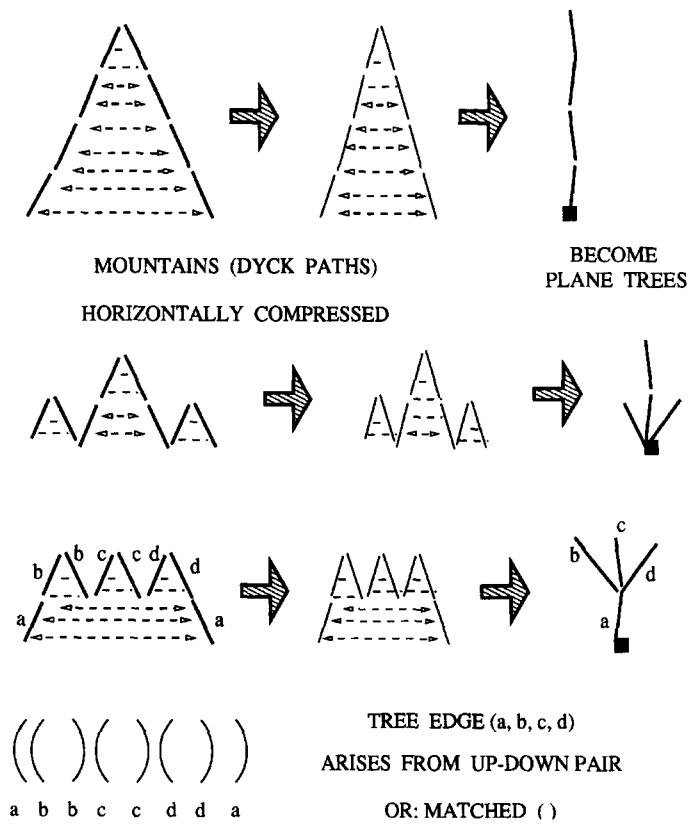


Fig. 9.

down, one square at a time. Each reachable square is to contain the number of different routes the king can take to get there.

The table is easily constructed. Put ones in the first row and zeroes immediately under the diagonal (obvious). Each square between will be seen to contain the sum of the numbers immediately left and immediately above. The main diagonal contains the Catalan sequence because the king may follow any Dyck path to reach it. A simple way to create this table, with readymade formulas will be given in Section 5. We may call this table the Catalan triangle (note [36]).

In Appendix C of [16] the Fine numbers are discussed; C.4 indicates how to find them in the Catalan triangle (the powers of function  $c(z)$  in [16] are in a sense the diagonals of the triangle). Finding  $C_5 = 42$  on the diagonal edge, and reading up gives the (column) 42, 42, 28, 14, 5, 1. A Fine number may be found (a) by an alternating sum, or (b) a sum of alternates:  $18 = 42 - 42 + 28 - 14 + 5 - 1, 57 = 42 + 14 + 1$ .

In Fig. 9 we imagine the mountainous outline to be physically realized as a strip of postage stamps with a wet and sticky under surface. If we compress the model horizontally, then each stamp pair representing matched parentheses is glued back to

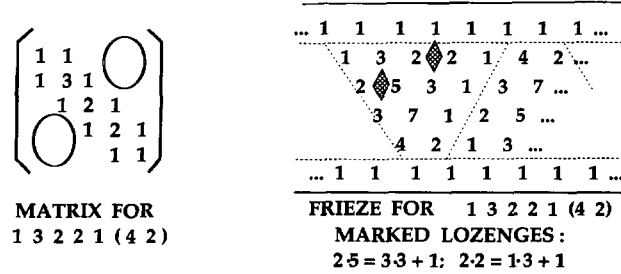


Fig. 10.

back. A planted plane tree results. Papers by Deutsch [16] and Chapman [12] provide many results on Dyck paths.

Our tour of Catalan families ends with a spectacular example. Take the deltoid in Fig. 3 with  $n = 6$  triangles (the octagon case). For vertices  $1, 2, \dots, 8$  write down the number of triangles concurring at these vertices, obtaining the sequence 33213321. This will be called the *margin* sequence of the deltoid.

If  $\mu$  is any subsequence formed by consecutive members of a margin sequence we define a matrix  $M(\mu)$  as a tridiagonal matrix, with determinant  $m(\mu)$ . This matrix has precisely  $\mu$  as its main diagonal, and ones above and below the main diagonal, and elsewhere zeros. The determinant has the following recursive rule.

$$m(\mu xy) = y \cdot m(\mu x) - m(\mu).$$

Fig. 10 shows  $M(13221)$  taken from a margin sequence 13221,42. It is an example of a class of positive definite matrices (see [38] for a fascinating account).

If  $u\mu v, xy$  is a margin sequence of length at least four, we have  $m(u\mu v)=1$ ,  $m(u\mu)=x$ , and  $m(\mu v)=y$ . From Fig. 10,  $m(13221)=1$ , and two principle minors are  $m(1322)=4$  and  $m(3221)=2$  (here delete either last row and column, or first row and column). The minor determinants compute the deleted numbers 4, 2!

Seeking a careful explanation, it is more fruitful to focus on a much richer pattern, a frieze [14]. A frieze is a pattern of positive whole numbers grouped into a finite stack of two-way infinite rows. The first and last rows are all ones, and the second and penultimate rows are endlessly repeating margin sequence  $\mu$ . In Fig. 10 a frieze  $F(1322142)$  is shown. The dashed lines outline a trapezoid which repeats; every other trapezoid has the order of the rows reversed. That is, the frieze has glide reflection symmetry.

The basic numerical rule is that any local ‘lozenge’ arrangement of four numbers in the frieze satisfies an equation: the horizontal product is one greater than the vertical product. In the diagram, two of these lozenges are marked, and the equations are displayed at the bottom.

It will be discovered that from this rule, the entire frieze may reconstructed from the second row, and again from any diagonal. A typical diagonal may be described as a sequence  $1, a, \dots, g, 1$  that contains positive whole numbers, begins and ends with one,

and has the further property that given any three consecutive elements  $x, y, z$ , the sum  $x + z$  is divisible by  $y$ . The reader may enjoy finding the quotient, which also appears in the ‘marginal’ second row.

The matrix connection is sealed by generalizing the following example. We take  $\mu = 3221$  from the 2nd row. This is upper side of a triangle whose other two sides are partial diagonals 3572 and 1112 meeting at bottom vertex 2. The bottom number (more generally any entry on or below row two of the frieze) is computed by  $m(3221)$  (more generally,  $\mu$  is the horizontal of a triangle, and  $m(\mu)$  is the bottom vertex).

The frieze, with its rich patterns is easier to handle with an inductive proof. A margin sequence 111 goes with a trivial frieze having only two rows: all ones. Given a frieze for margin sequence  $\mu = \dots, x, y, \dots$  just do the tedious check of what happens to all the properties in passing to  $\mu' = \dots, x + 1, 1, y + 1, \dots$ .

### 3.2. Recurring numbers: Riordan

Next we list three counting problems similar to the above, but which lead to numbers  $R_n$ . Table 2 shows the three families.

#### [R1] Tall (or short) bushes

A tall (short) bush is a plane tree in which the root has degree one (more than one) and no vertex (no non-root vertex) has degree two. Shrinking the ‘stalk’ converts a tall bush into a short bush. More generally, this transformation turns planted trees into potted trees. The number  $R_n$  counts the tall bushes with  $n + 1$  edges, or the short bushes with  $n$  edges. Since all bushes with  $n + 1$  edges are counted by  $M_n$  (see the next section) we anticipate the result  $M_n = R_n + R_{n+1}$ .

#### [R2] Cyclically spaced (or feasible) noncrossing partitions

In the following, the simpler terms *feasible* and *infeasible* will replace the cumbersome terms cyclically spaced and noncyclically spaced. These terms are suggested by the idea of a partition which generates a feasible coloring of a circuit graph. A feasible partition which is also noncrossing then corresponds to the planar colorings of Tutte. (‘Cyclically spaced’ and ‘noncrossing’ were defined in Section 2.)

#### [R3] Noncrossing partitions with no singletons

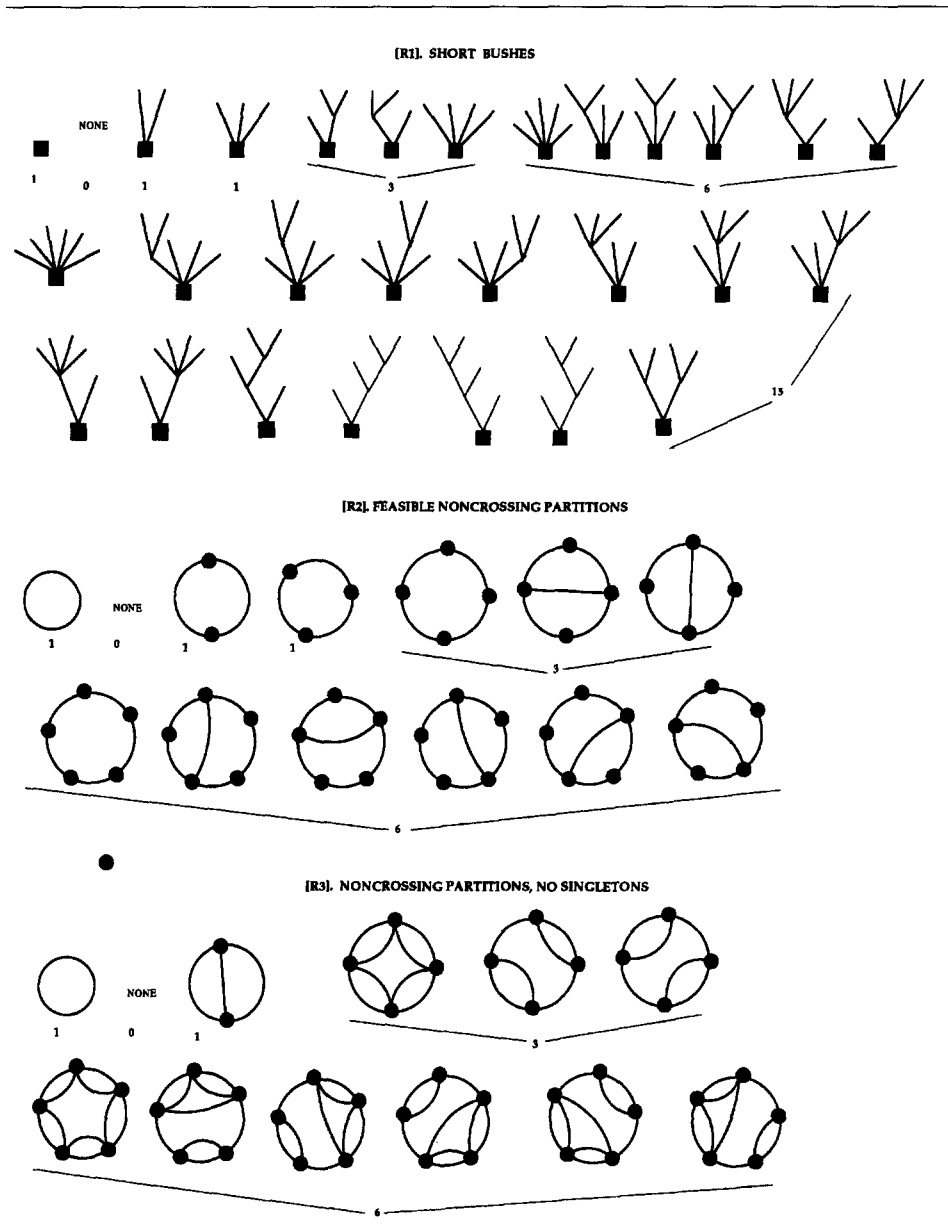
This is the class of NC partitions such that every class has at least two members.

It was pointed out in Section 2.3 that every NC partition has a dual NC partition. It is readily seen that a vertex is a singleton in the former just in case the corresponding pair of adjacent vertices of the dual are joined. Hence there is an elegant correspondence between the families [R2] and [R3].

We still need a correspondence between [R1] and either [R2] or [R3]. This is so closely linked with the Motzkin numbers that we postpone dealing with it until Section 2.4.

Consider for a moment the class of all partitions of  $n$  points on a circle (all partitions of an  $n$ -set). The number of these is the Bell number  $B_n$  [M1484]. Let  $V_n$  be the number of cyclically spaced (feasible) partitions and let  $W_n$  be the number of partitions without singletons. Surprisingly,  $V_n = W_n$  [M3423] and even more remarkably,  $B_n = V_n + V_{n+1}$ !

Table 2  
Riordan (RING) families



The analogy with  $C_n, M_n, R_n$  seems to be that removal of the NC restriction substitutes  $B_n$  for both  $C_n, M_n$  and substitutes  $V_n$  for  $R_n$ . We note that the exponential generating functions [47] for  $B_n, V_n$  are

$$B(x) = \exp(\exp(x) - 1), \quad V(x) = \exp(x)(\exp(x) - x - 1).$$

Inspection of these functions easily shows that (for derivative  $V'(x)$ )

$$B(x) = V(x) + V'(x) \quad \text{from whence } B_n = V_n + V_{n+1}.$$

A table for these sequences was given in the introduction.

The most tempting approach to the generalization is to broaden the concept of duality to cover the nonplanar cases. Unfortunately, this does not seem to work; there is apparently no simple way to bring the sets counted by  $V_n$  and  $W_n$  into one-to-one correspondence!

Amazingly, the equations  $B_n = V_n + V_{n+1}$  and  $B_n = W_n + W_{n+1}$  can be justified with a combinatorial correspondence! (These correspondences are given in Section 3.5. Since  $V_0 = W_0 = 1$ , it follows that the cyclically spaced  $n$ -point partitions are equinumerous with the  $n$ -point partitions without singletons! Indeed, the combined set of feasible partitions for  $n$  and  $n + 1$  can be transformed into the combined set of partitions without singletons for  $n$  and  $n + 1$ . This is very peculiar since the correspondence does not observe the distinction between  $n$  and  $n + 1$ . Attempts to repair the correspondence do not appear to bear fruit.

There is a standard recursion for  $R_n$  analogous to the standard recursion for the  $C_n$  (last section) and the standard recursion of the  $M_n$  (next section). It is

$$R_{n+1} + (-1)^n = R_0R_n + R_1R_{n-1} + \cdots + R_nR_0.$$

A simple decomposition which explains it is given in the section Appendix 3.4. The equation that defines power series coefficients for  $y = \sum_{n=0}^{\infty} R_n x^n = 1 + 0x + x^2 + \cdots$  by this recursion is

$$y = \frac{1}{1+x} + xy^2.$$

### 3.3. Recurring numbers: Motzkin

Motzkin numbers are one of several number sequences introduced in 1948 [27] by Motzkin and are aptly named because they count almost as many things as Catalan numbers [20]. Here are three situations in which Motzkin numbers arise (Table 3).

#### [M1] *Noncrossing (NC) partial pairs*

Out of  $n$  points on a circle, an even subset, possibly empty, is paired as in [C2].

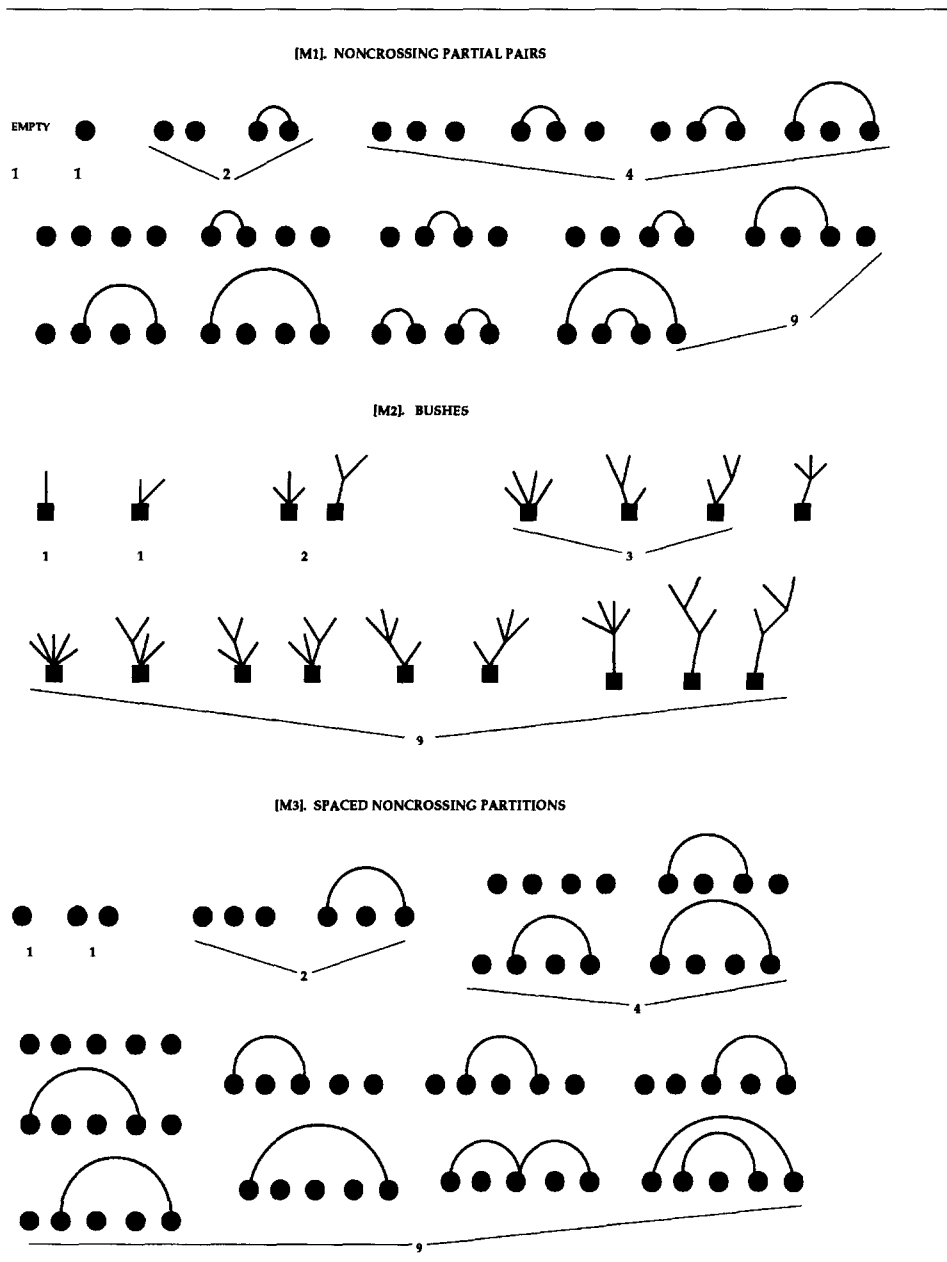
This is basically the Motzkin definition. Table 3 shows this family in row diagram form. Note the fifteen point example of Fig. 11. Scan the row from left to right and assign each point the label + (for +1) if it is the left end of an arc, - (for -1) if it is the right end, and 0 if it is isolated. This produces a (+0-) pattern.

#### [M2] *Plane bushes*

The plane bushes with  $n + 1$  edges are counted by  $M_n$ .

It is clear that bushes with  $n + 1$  edges may be divided into two subclasses: the short and the tall (these subclasses will soon be called upper and lower, respectively). Hence  $M_n = R_n + R_{n+1}$ , due to class [R1].

Table 3  
Motzkin families



[M3] *Strict feasible noncrossing (NC) partitions*

A feasible (i.e. cyclically spaced) NC partition is a *strict partition* if the first point ( $v_1$  say) is a singleton: in a class by itself. Then  $M_n$  counts the strict partitions of  $n+2$  points on a circle.



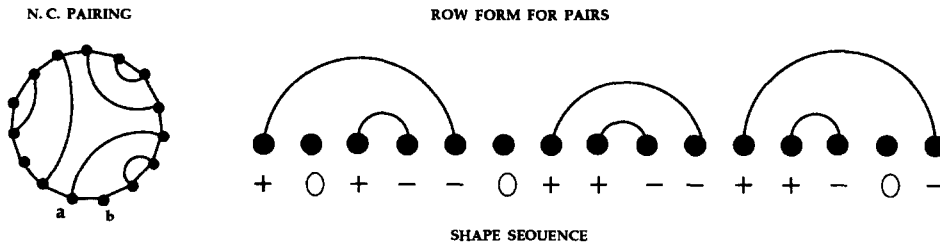


Fig. 11.

Take a strict partition on  $n$  vertices, and delete the leftmost point. This results in the variation found in Table 3. Following D. G. Rogers, these are called the *spaced* NC partitions. Each spaced NC partition is one of (a), (b):

- (a) a feasible NC partition [R2] on  $n - 1$  points, or
- (b) an almost feasible NC partition (the endpoints are joined).

In (b) we just delete an endpoint to get a feasible NC partition on  $n - 2$  points. Referring to [R2] we conclude that  $M_n = R_n + R_{n+1}$ .

Now we begin to compare families. Already the equation  $M_n = R_n + R_{n+1}$  has been manifested by a decomposition of families [M2] and [M3] into ‘upper’ and ‘lower’ Riordan classes. What about [M1]? The required decomposition is easiest using the  $(+0-)$  pattern. Classify the pattern as ‘upper’ if the first label different than PLUS is ZERO, ‘lower’ if it is MINUS. We show how to collapse the lower class of level  $n$  onto the upper class of level  $(n - 1)$ : replace the leftmost  $(+, -)$  pair by a zero. The zero will also be the first zero.

Now we describe how to convert [M1] to [M3]. Add a new point at the right end of the row diagram. Take each arc that connects a pair and move the right hand end one point further to the right. This converts a partial pairing of  $n$  points to a spaced NC partition of  $n + 1$  points. Curiously, this does not put the upper and lower subclasses into agreement.

We may also convert [M2] to [M3] by a method which simplifies Prodinger [28]. Take a potted tree and put a letter on each edge, with the proviso that the rightmost upward edge, for any nonroot vertex  $x$  with more than two edges, has the same label as the edge at  $x$  preceding backward towards the root. This is the only time that labels are repeated.

From the root describe a clockwise tour around the bush and collect all the labels (the label is collected at first opportunity). This process is easy to do visually (Fig. 12) when the label is written on the left side of the edge. The sequence is the scheme for an NC partition. In fact, we have a bijective mapping from Catalan class [C3] and potted trees.

Inspection easily shows that requiring the tree to be a bush is exactly what is necessary and sufficient to avoid repeats  $\dots xx \dots$  in the scheme. Thus bushes correspond

FROM PLANE TREES TO NC PARTITIONS

EDGE LABELS ON LEFT SIDE, LABELS OF RIGHTMOST EDGES REPEAT  
 COLLECT LABELS IN SEQUENCE BY CLOCKWISE (PREORDER) TOUR

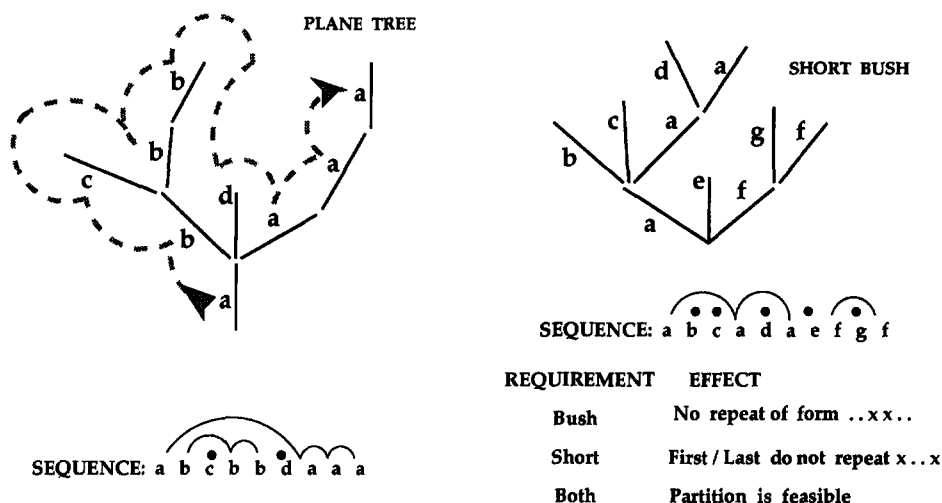


Fig. 12.

to spaced partitions. Moreover, limiting to short bushes avoids a repeat  $x \dots x$ , and so makes a matching between short bushes and feasible partitions.

At this point all three  $M$ -families are seen to be equinumerous. Since each family has a suitable upper/lower  $R$ -decomposition and since  $M_0 = R_0 = 1$  may be verified in all three cases, it follows that the equation  $M_n = R_n + R_{n+1}$  harmonizes with all cases (no different definition of  $R_n$  is needed).

A different approach involves the standard Motzkin number recursion

$$M_{n+2} - M_{n+1} = M_0 M_n + M_1 M_{n-1} + \dots + M_n M_0.$$

The decomposition needed to show that an  $M$ -family [Mi] agrees with this recurrence is as follows: first, an ‘inner’ subclass of level  $n + 2$  which collapses onto level  $n + 1$ , and a decomposition paralleling the Catalan decomposition for the remaining ‘outer’ subclass.

Take [M1]. If the first point  $v_1$  is isolated, remove it. This exhibits the collapsing inner subset. On the other hand, suppose that  $v_1$  is joined to  $v_k$ . Then the possibly empty ranges  $v_2, \dots, v_{k-1}$  and  $v_{k+1}, \dots, v_{n+2}$  define numbers of smaller families on levels  $k - 2$  and  $n - k + 2$  (Fig. 13A).

Take family [M3] next. Start with a spaced NC partition of  $n + 3$  points. The collapse of the inner class is defined by deleting the first point  $v_1$  when it is isolated. Otherwise suppose that  $v_k$  is the first point in  $v_3, v_4, \dots$  joined with  $v_1$ . The non-empty ranges  $v_2, \dots, v_{k-1}$  and  $v_k, \dots, v_{n+3}$  define the decomposition, as shown in Fig. 13B.

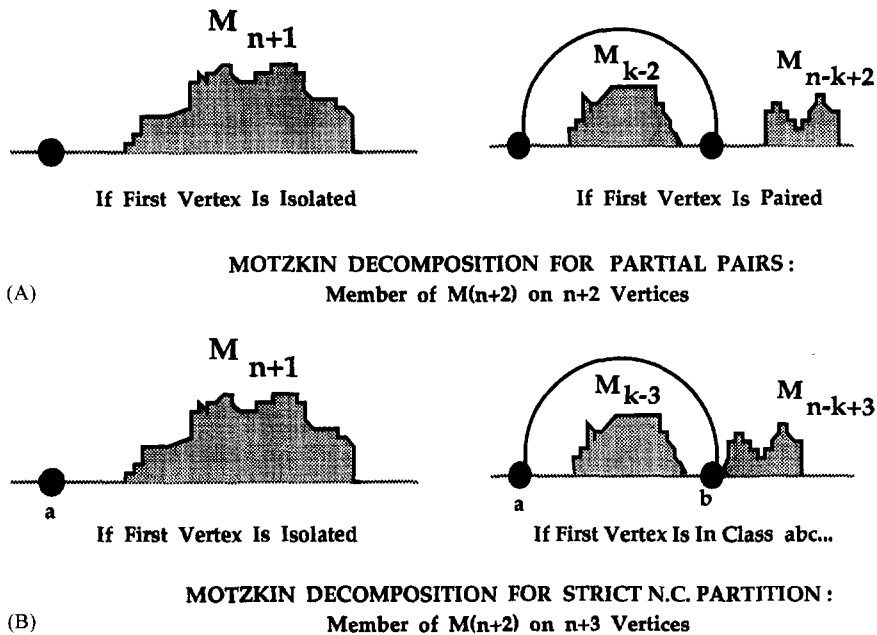


Fig. 13.

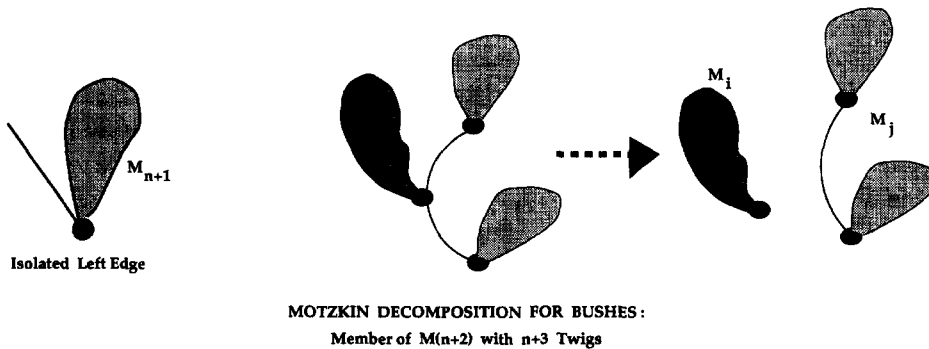


Fig. 14.

Finally, take family [M2] and refer to Fig. 14. Remove the leftmost edge at the root if it ends in a tip only, leaving a member of level  $n - 1$ . Otherwise, let the bush indicated by the dark shading (a member of level  $i$ ) be plucked off. The attachment point disappears and another bush is left from level  $j$ .

Since all three families [M1–M3] have such a standard decomposition, and agree with  $M_0 = 1$ , we have another combinatorial demonstration that all families generate the same numbers. Moreover, there is an implicit promise in the combinatorial method that one-one correspondences are possible — in fact we have already showed  $[M1] \Leftrightarrow [M3]$ ,  $[M3] \Leftrightarrow [M2]$  in this way. The implicit promise can be made explicit as follows.

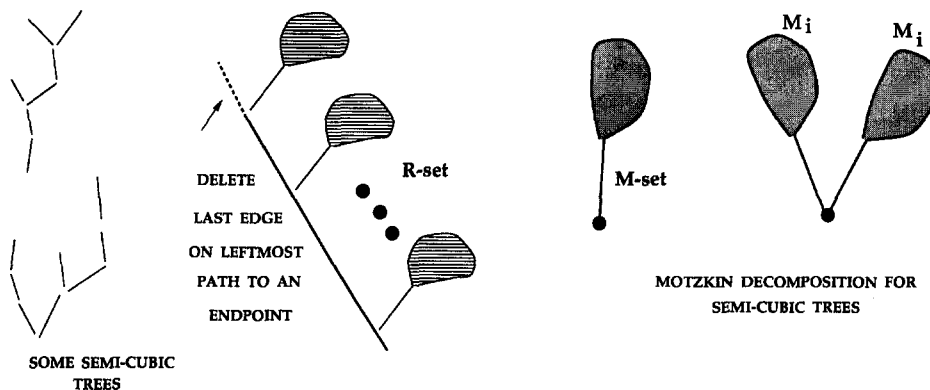


Fig. 15.

Once a standard  $M$ -decomposition has been established for a family, a history tree can be developed for any member ( $X$  say). Either  $X$  is in the inner class and collapses to  $X'$  (say), or it decomposes in Catalan fashion into a pair  $(X_i, X_j)$ , or it is the trivial member of level zero. Let the trivial tree of no edges do for the last. In the first case let a stalk from the root be given and attach the history tree for  $X'$  at the top. In the second case, let there be two edges at the root and put the trees for  $X_i, X_j$  on the left and right edges (see Fig. 15).

Carrying out this process leads to an interesting variation on the planted trees. A *semi-cubic tree* or SCT is a plane tree in which each vertex has degree at most three and the root at most two. Let the rightmost upwards edge at any vertex, if any, slant to the right. Let the second edge, if any, slant to the left. The class of SCTs most visibly embodies the standard decomposition.

But what about the upper/lower? An SCT belongs in the collapsing R-set if the leftmost path from root to tip includes only left slanting edges. It is collapsed by removing the last one of these (middle of Fig. 15).

A standard decomposition for an  $M$ -family is in effect a mapping of the family onto the semicubic trees. Thus any two families with  $M$ -decompositions are at least in indirect correspondence. Conversely, if two families are in direct correspondence, an  $R$ -decomposition or an  $M$ -decomposition for one can usually be transferred to the other.

These families and many more counted by  $M_n$  are listed by Donaghey and Shapiro [20]. They include bushes as #8 and semicubic trees as #13. Their family #3, planted trees with loops, can be put into simple correspondence with M1 (see Fig. 16). They do not use one-to-one correspondences throughout, but the interested reader should try out the methods above on their families.

A very recent paper [3] must be mentioned. In it there are a large number of beautiful relationships presented between Riordan numbers, Motzkin numbers, and other sequences encountered below in Section 4.

Consider again the transformation [M1] to [M3], by stretching the arcs. The reverse transformation applies to spaced NC partitions; what if we apply it to an arbitrary NC

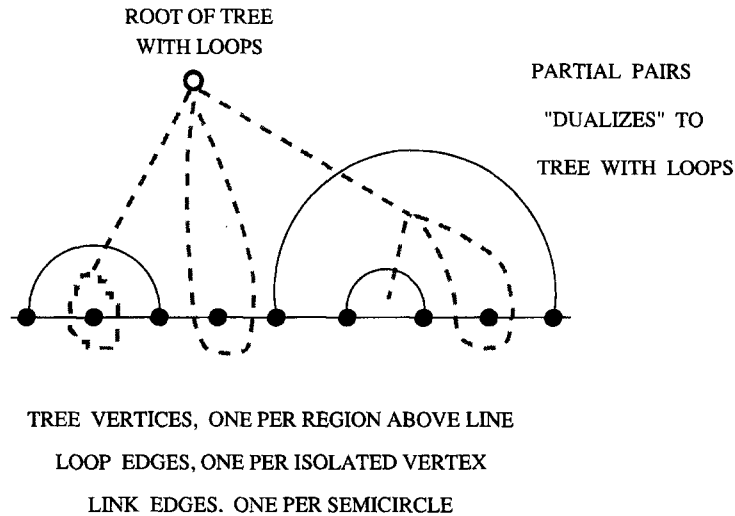


Fig. 16.

partition? In that case an arc joining points  $i, i + 1$  flattens to a loop on point  $i$ . Hence another Catalan family is given by allowing singleton vertices of the partial pairs [M1] to have loops. Put differently, select out of  $n$  points  $2i$  to be paired, and color the rest red (no loop) or green (loop). This yields a beautiful formula of Touchard [37]:

$$C_{n+1} = \sum_i \binom{n}{2i} 2^{n-2i} C_i.$$

### 3.4. Appendix on $R$ -recursion

Recall the standard  $R$ -recursion  $R_{n+1} + (-1)^n = R_0 R_n + R_1 R_{n-1} + \dots + R_n R_0$ . What sort of  $R$ -class decomposition is needed to justify it? Evidently a Catalan-like decomposition is desired, but with irregularities. We handle these by defining certain singular bushes in the family of short bushes.

Let  $b_0$  be the trivial tree/bush with no edges. Let  $b_2$  be the tree/bush with two edges at the root (the letter 'V'!). Let  $b_{2k+2}$  be the bush obtained by attaching  $b_{2k}$  to the top of the left edge of  $b_2$ . In other words,  $b_{2n}$  is a stack of  $n$  V's, leading to the left. These bushes will be called exceptional (Fig. 17A).

Consider the short bushes with  $n + 1 > 0$  edges. Member  $X$  is to be decomposed into  $X_i$  and  $X_j$  with  $i$  and  $j$  edges, respectively, where  $i + j = n$ . But if  $X$  is exceptional, then no decomposition is given and all pairs  $(X_i, X_j)$  occur, except for  $(b_{2k}, b_0)$ , which cannot occur. The former applies when  $n$  is even; the latter when  $n$  is odd. This will fill the bill, if we succeed.

Fig. 17B shows the decomposition schematically. Bush  $B$  (dark shading) is possibly trivial, but bush  $C$  cannot be. A pair of arrows point downward to  $X_i$  and horizontally to  $X_j$ . The horizontal action as long as  $X_i$  is trivial may be described as a piston-like

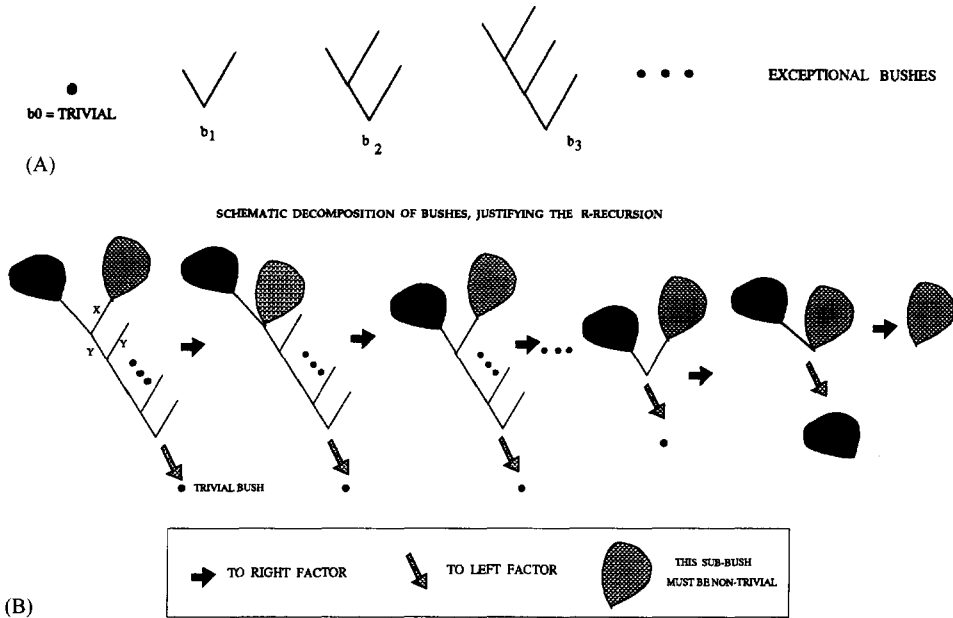


Fig. 17.

motion of  $C$ : an inward thrust eliminates one edge and an outward thrust removes one V-edge-pair from the lower body. The last step pictured is the standard Catalan decomposition for potted trees; here it applies when  $X$  is a bush with more than two edges at the root, the only case which guarantees  $C$  to be a short bush.

Verification that all non-exceptional bushes  $X$  have a unique decomposition, and that each pair  $(X_i, X_j)$  different from  $(b_{2k}, b_0)$  occurs once is left to the reader.

### 3.5. Appendix on Bell decomposition

We promised to show that  $B_n = V_n + V_{n+1}$  in two ways. Let  $b_n, v_n$ , stand for the set of all partitions of  $(1, 2, \dots, n)$ , and the subset without singletons. Since  $v_n$  is a subset of  $b_n$ , we look for a correspondence of  $v_{n+1}$  with  $b_n - v_n$ . Take a partition  $\pi$  in  $v_{n+1}$  and break the class containing  $n + 1$  into singletons (more than one) and delete  $n + 1$ . For example, using schemes,  $abcccbac \rightarrow abxxxba \rightarrow abcdeba$ .

The other correspondence is similar, but for a big pothole. Let  $W_n$  count the feasible partitions, forming set  $w_n$  already a subset of  $b_n$ . But we do not map this subset to itself ! (This avoids the pothole.) Rather, annex new member  $n + 1$  to the class containing 1, arriving at  $w'_{n+1}$ . The union of  $w'_{n+1}$  and  $w_{n+1}$  is disjoint, and yields the spaced partitions of  $(1, 2, \dots, n)$ . Given a spaced partition in this union, break the class containing  $n + 1$  into elements, delete  $n + 1$ , but annex each other element  $i$  to the class containing  $i + 1$ . For example,  $abacbc \rightarrow abaxb \rightarrow ababb$ , and  $abcbad \rightarrow abcba$ .

#### 4. CMR tossed salad

Recall that each member of Motzkin family [M1] defines a (+0−) sequence. Each arc joins a left point marked + to a right point marked −. Isolated points are marked 0. It will always be the case that if the sequence is added from left to right (where +, −, 0 are taken as +1, −1, 0) no sum will be negative and the final total will be zero. Any (+0−) sequence which obeys these rules is a *Motzkin shape*. Conversely, every Motzkin shape defines a member of [M1]. Details of those proof make an easy exercise.

Consider a pair of row vectors  $A, B$ , containing ones and zeros only. We will assume that  $A, B$  have the same length, and the difference  $A - B$  is a Motzkin shape (implying that both rows have the same number of ones). The shape does not determine the pair  $A, B$  unless we distinguish between ‘thick’ zeroes  $1 - 1$  and ‘thin’ zeroes  $0 - 0$ . For definiteness, modify a Motzkin shape to a  $*$ -shape by changing some, all, or none of the zeroes to  $*$ , where  $*$  means a thick zero, and 0 is a thin zero. From this shape the pair  $A, B$  may be recovered. By interpretation, we have two-colored the zeroes, and therefore the number of  $*$ -shapes is a Catalan number (see the end of Section 3.3).

Assign the components of  $B$  to the top row and the components of  $A$  to the bottom row of a 2-by- $n$  arrangement of dots. Construct a graph by joining the first plus of the bottom row to the first in the top row, then the second to the second, and so on. No edge will cross or meet another edge, and no edge will have negative slope. This graph is called an increasing bipartite graph, or IBG [20].

A Motzkin shape then determines a thin IBG, which has only thin zeroes, and also a thick IBG, which has only thick zeroes (interpret each 0 as  $*$ ). Moreover, the row diagrams of family [M1] can be considered as thin interpretations of Motzkin shapes. And so there will be a matching thick interpretation, where each 0 is the right-hand end of one arc and the left-hand end of another. Strictly understood, some zeroes will then have loops; however, it is possible to remove or ignore them.

The thin row graphs are just the row forms of the family [M1]. The thin IBG is a graph with at most one endpoint (+1 in the matrix interpretation) per column. The thick IBG, on the other hand, is characterized as an IBG in which every column meets an edge.

That leaves the thick row diagram to explain. It is a NC partition in which no singleton is ‘covered’. More simply, append one more point to the beginning of the row, and then chain together the singletons. The result is a NC partition with no singletons, except possibly the first point. This Motzkin family was encountered in Section 2.3.

There are a large number of IBG Motzkin families. Indeed, the following transformations can be used to generate one from another:

(T1) Turn the matrix (or the IBG) upside down; that is, exchange the rows  $A, B$  and reverse the order within each row.

(T2) Exchange the rows and exchange (0, 1) elementwise.

(T3) Append zeroes to the beginning of row  $B$  and the end of row  $A$ .

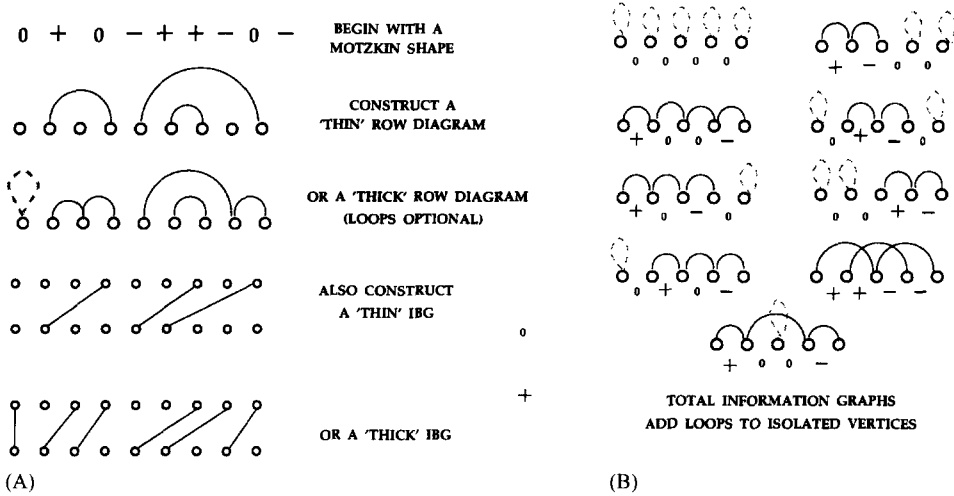


Fig. 18.

(T4) Append ones to the beginning of row  $A$  and the end of row  $B$ .

(T5) Delete or add a constant column to the left or the right side of the matrix.

The thick and thin IBG families illustrated above are left fixed by (T1), and exchanged by (T2). (T2) and (T4) combined are a case of (T5): adding a column of ones at the end and adding a column of zeroes at the beginning.

Table 4 shows a number of IBG families illustrated for the case  $M_4 = 9$ . The third group is the same as family #7 from [20] is the IBG in which the isolated points (non-endpoints) in row  $A$  are nonadjacent, or spaced out. The Motzkin shape sequence may be recovered as follows. First add a column of ones (a final vertical edge). Label each isolated point in the top row with +. Label each endpoint in the top row with - if the other end immediately follows an isolated point: otherwise label it 0.

Consider the row diagrams of Fig. 18B. Isolated vertices have loops (optionally visible). A pair  $x, y$  of adjacent vertices satisfy the following rule:  $x$  has a loop only or is the right end of an arc,  $y$  has a loop only or is the left end of an arc, or both the above. The three cases are marked -, +, 0 to get a Motzkin shape.

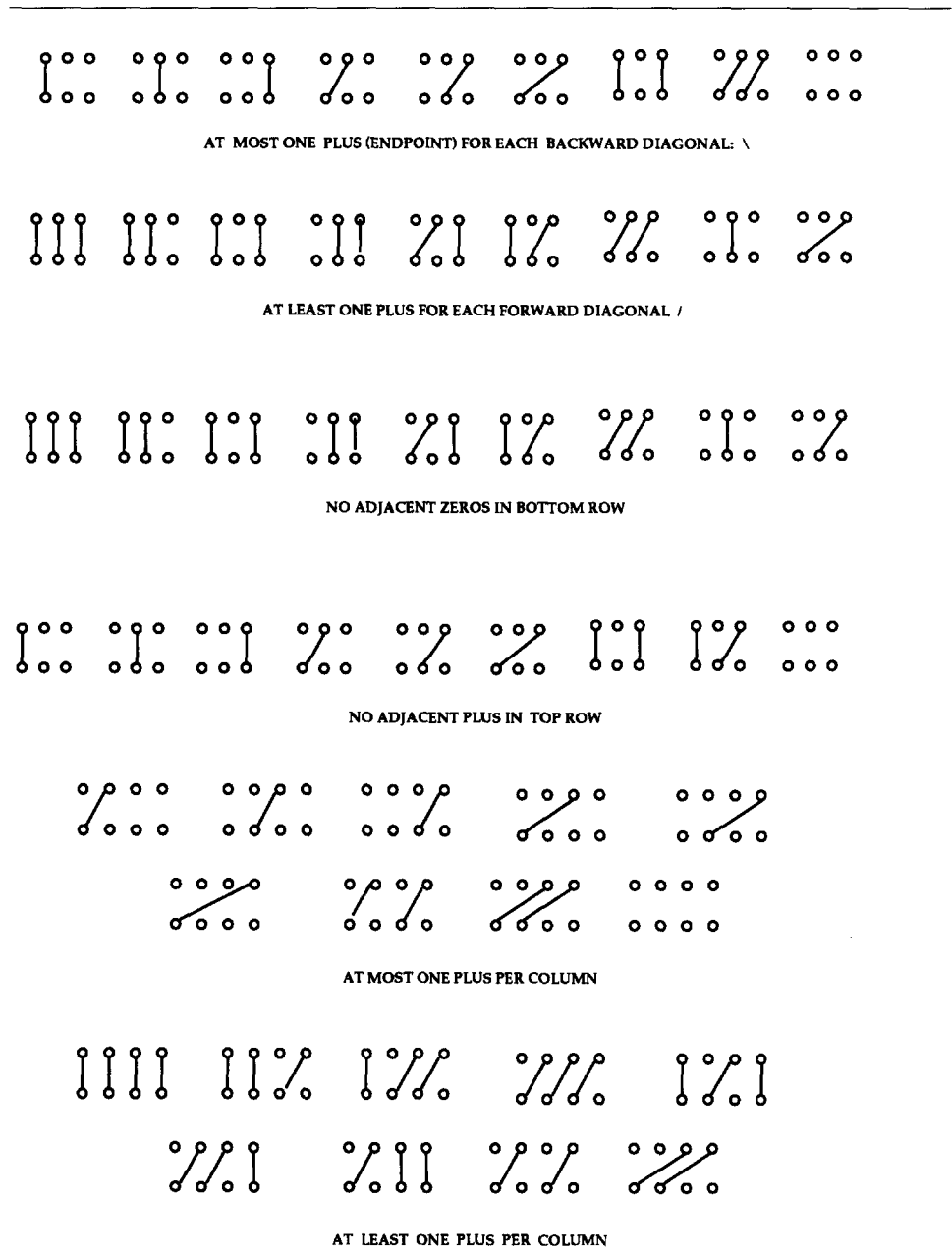
An interesting interpretation is as follows. The vertices represent an increasing set of weights. A certain weak balance is used to test pairs of weights with the possible outcome that one weight is heavier, or the two are too close to call. The graph arcs connect the ends of the maximal intervals of similarity. Row diagrams according to the above rules are Total Information graphs, permitting the correct order of the weights to be determined. Natural consistency rules apply to the balance [38].

Each IBG can also be rendered as a lattice path. Suppose that  $(a_i)$  and  $(b_i)$  record the positions of the pluses in the lower and upper rows, respectively, for  $i = 1, 2, \dots, k$ . Then there is a lattice path made of straight segments joining the successive points

$$(0, 0), (b_1, 0), (b_1, a_1), (b_2, a_1), (b_2, a_2), \dots, (b_k, a_{k-1}), (b_k, a_k), (n + 1, a_k), (n + 1, n + 1).$$



Table 4  
IBG families ( $M_4 = 9$ )



Each family of IBGs can thus be transformed into a family of lattice paths. In Fig. 19 the upward diagonal is the  $X$ -axis, and the downward diagonal is the  $Y$ -axis, in order that we can recognize a lattice path as another form of mountain range.

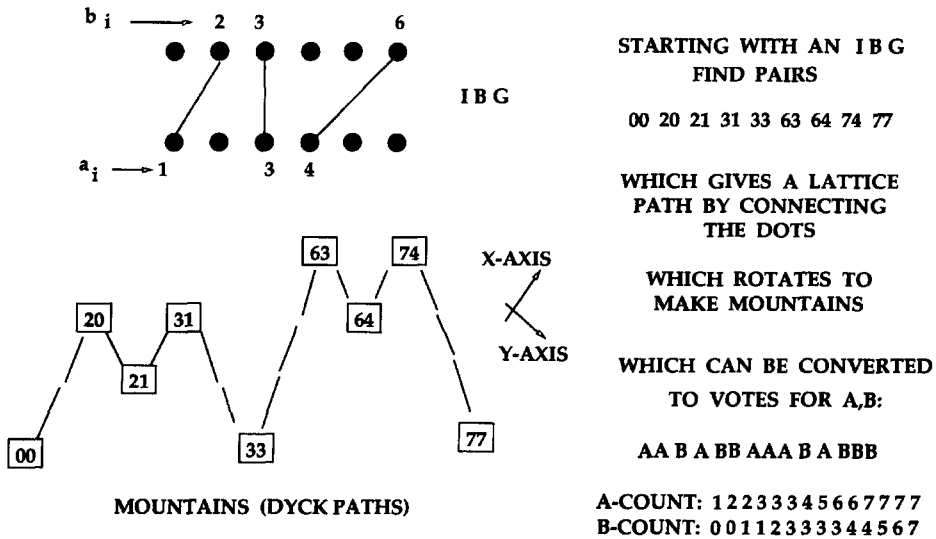


Fig. 19.

Each lattice path can in turn be rendered as a ballot sequence. A vote for candidate *A* means an edge in the lattice graph directed from  $(i, j)$  to  $(i + 1, j)$ , and a vote for candidate *B* means an edge directed from  $(i, j)$  to  $(i, j + 1)$ . Here candidate *A* never falls behind *B* as the sequence is counted, but the end result is a tie.

The systematic application of these transformations will bring the ballot sequences, lattice paths, and increasing bipartite graphs into close relationship. The reader may wish to examine the Motzkin families found in [20] passed over here, in order to make explicit *R*-decompositions and *M*-decompositions for them. When this is completed, all the Motzkin families described there and here will be brought into combinatorial correspondence.

If the zeroes are deleted from a Motzkin shape sequence, a possibly empty sequence of plus and minus remain. As seen by comparing families [C2] and [M1], such a sequence describes a Catalan pairing. Hence the formula

$$M_n = \sum_k \binom{n}{2k} C_k.$$

### 5. The difference it makes

Consider the NC partitions counted by  $C_n$ . A particular vertex is a witness (to feasibility) if it is not joined to the immediately following vertex by the partition (point 1 follows point  $n$ ). Call a NC partition *k*-feasible, for  $k = 0, 1, 2, \dots, n$  if the first *k* points are witnesses. Thus, every NC partition is 0-feasible and only the feasible NC partitions are *n*-feasible.

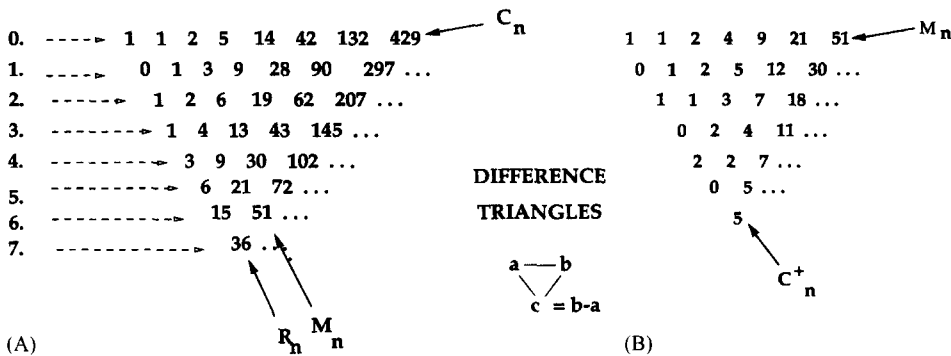


Fig. 20.

If  $a, b, c, d, \dots$  is the sequence which counts  $k$ -feasible NC partitions for  $n=k, k+1, \dots$ , then the sequence which counts  $(k+1)$ -feasible NC partitions for  $n=k+1, k+2, \dots$  is easily found to be  $b-a, c-b, d-c, \dots$ . For, an  $n$ -noncrossing partition which is  $k$ - but not  $(k+1)$ -feasible is converted to a  $k$ -feasible NC partition of  $n-1$  points by merging point  $k+1$  with the following point. It follows that a difference triangle may be constructed starting with the  $C_n$  as shown in Fig. 20A.

Each row gives the differences of the row above and is indented further. Clearly, the  $k$ -row gives the  $k$ -feasible partitions for  $n=k, k+1, \dots$  points and, therefore, the first diagonal  $(1, 0, 1, 1, 3, 6, \dots)$  gives the number of feasible partitions, which we know to be  $R_n$ . The second diagonal  $(1, 1, 2, 4, \dots)$  is the Motzkin sequence, since  $M_n=R_n+R_{n+1}$  and also because the spaced partitions of  $n$  points are just the  $(n-1)$ -feasible partitions.

If a difference triangle begins with row  $a_0, a_1, a_2, \dots$ , then formulas for other rows and diagonals are most convenient with the shift operator  $E(a_i) = a_{i+1}$ . The  $k$ th row after the first is

$$(E - 1)^k(a_i) = \sum_j (-1)^{k-j} \binom{k}{j} (a_{i+j}).$$

Thus, we have

$$R_n = \sum_i (-1)^{n-i} \binom{n}{i} C_i, \quad M_n = \sum_i (-1)^{n-i} \binom{n}{i} C_{i+1}.$$

The roles are reversed by using  $E + 1$  instead of  $E - 1$ .

$$C_n = \sum_i \binom{n}{i} R_i, \quad C_{n+1} = \sum_i \binom{n}{i} M_i.$$

One other difference triangle is noteworthy. (See Fig. 20B.) It puts Motzkin instead of Catalan numbers on the initial row. The first diagonal is the ‘aerated’ Catalan sequence:

$$C_n^+ : 1, 0, 1, 0, 2, 0, 5, 0, 14, 0, 42, 0, \dots$$

There are two connection formulas it represents:

$$C_n = \sum_i (-1)^{2n-i} \binom{2n}{i} M_i, \quad M_n = \sum_i \binom{n}{2i} C_i.$$

The second formula is certainly correct because we know that one way to construct members of family [M1] for  $n$  points is to select  $2i$  points to be paired in  $C_i$  possible ways, It follows that the diagonal really is  $C_n^+$  and the other formula is correct also. We also see that the second diagonal repeats every Catalan number twice after the first (the ‘stuttering’ Catalan sequence??).

Discarding the first diagonal and reapplying the connections yields still other formulas. A number of such CM connections are studied by Donaghey [18].

Combining the C-M and the M-C connections from both difference tables gives a Catalan recursion formula of interest:  $C_{n+1} = \sum_{i,j} \binom{n}{i} \binom{i}{2j} C_j$ . The substitutions

$$\binom{n}{i} \binom{i}{2j} = \binom{n}{2j} \binom{n-2j}{i-2j}, \quad \sum_i \binom{n-2j}{i-2j} = 2^{n-2j}$$

transform it quickly to a beautiful formula we have seen already (Touchard)

$$C_{n+1} = \sum_i \binom{n}{2j} 2^{n-2j} C_j.$$

## 6. Count on it

### 6.1. Catalan–Motzkin–Riordan enumerators

We have seen the following characteristic equations in previous sections:

$$\begin{aligned} y = C: & \text{ Catalan } (1, 1, 2, 5, 14, 42, \dots) \quad y = 1 + xy^2, \\ y = M: & \text{ Motzkin } (1, 1, 2, 4, 9, 21, 51, \dots) \quad y = 1 + xy + x^2y^2, \\ y = R: & \text{ Riordan } (1, 0, 1, 1, 3, 6, 15, 36, \dots) \quad y = \frac{1}{1+x} + xy^2. \end{aligned}$$

In the first of these one may put  $x^2$  for  $x$  to get

$$y = C^+: \text{ aerated Catalan } (1, 0, 1, 0, 2, 0, 5, 0, \dots) \quad y = 1 + x^2y^2.$$

Given only one of the enumerators, the others can be recovered using the difference triangles. Suppose a difference triangle has for top row the coefficients of  $A(x)$ , for the first diagonal the coefficients of  $B(x)$ , and for the second diagonal the coefficients of  $D(x)$ . Then  $A, B, D$  are related by the following Euler transformations:

$$(1+x)B(x) = A\left(\frac{x}{1+x}\right), \quad (1+x)B(x) = xD(x) + b_0.$$

For instance, let  $y = A(x) = C(x)$ ; then

$$\begin{aligned} C(x) &= 1 + xC^2(x), \\ C\left(\frac{x}{1+x}\right) &= 1 + \frac{x}{1+x}C^2\left(\frac{x}{1+x}\right), \\ (1+x)R(x) &= 1 + x(1+x)R^2(x), \end{aligned}$$

and similarly for the other cases. The characteristic equation  $y = 1 + xy^2$  for  $C(x)$  yields by implicit differentiation  $y' = y^2 + 2xyy'$ . Algebraic manipulation of the two equations yields the linear differential equation  $1 + (2x - 1)y + (4x - 1)(xy') = 0$ . This gives the ‘quick’ recursion

$$C_n = 2 \frac{2n - 1}{n + 1} C_{n-1}.$$

A similar straightforward but arduous manipulation of the  $R$ -equation leads to the linear equation  $1 - x(1 + x)(1 - 3x)y' = (1 - 3x^2)y$ . From the  $M$ -equation we obtain  $(2 - 3x - 3x^2)y + x(1 - 2x - 3x^2)y' = 2$ . The resulting quick recursions are

$$R_n = \frac{n - 1}{n + 1} (2R_{n-1} + 3R_{n-2}), \quad M_n - M_{n-1} = \frac{n - 1}{n + 2} (M_{n-1} + 3_{n-2}).$$

Fans of the quadratic formula may prefer to apply it to the characteristic equations to obtain

$$C: 2xy = 1 - \sqrt{1 - 4x}$$

(hence, by binomial expansion,  $C_n = \frac{2^n}{(n+1)!} 1 \cdot 3 \cdots (2n - 1) = \frac{1}{n+1} \binom{2n}{n}$ ), and

$$M: 2x^2y = 1 - x - \sqrt{1 - 2x - 3x^2},$$

$$R: 2x(1 + x)y = 1 + x - \sqrt{1 - 2x - 3x^2}.$$

Some interesting related facts are

$$\sqrt{1 - 4x} = 1 - 2x(C_0 + C_1x + C_2x^2 + \cdots),$$

$$\frac{1}{\sqrt{1 - 4x}} = \sum_n (n + 1)C_n x^n = \sum_n \binom{2n}{n} x^n,$$

$$\sqrt{1 - 2x - 3x^2} = 1 - x - 2x^2(M_0 + M_1x + M_2x^2 + \cdots),$$

$$\begin{aligned} 1/\sqrt{1 - 2x - 3x^2} &= \sum_n (1 + 2M_0 + 4M_1 + \cdots + 2(n - 1)M_{n-2})x^n \\ &= 1 + x + 3x^2 + 7x^3 + 19x^4 + 51x^5 + \cdots. \end{aligned}$$

Here the sequence 1, 1, 3, 7, 19, 51, ... or the constant terms of  $(\frac{1}{x} + 1 + x)^n$ , is seen again below.

### 6.2. Inversion to the rescue

The difficulties which beset the attempt to find closed form solutions for  $M_n, R_n$  can be overcome using Lagrange inversion. This is a very powerful tool which is naturally suited to many enumeration problems. There are several forms of the inversion theorem, including some generalizations which will not be needed here. Two closely related versions will be stated. Proofs using several methods can be found in [23].

TANNENBAUM (TRINOMIAL TABLE)

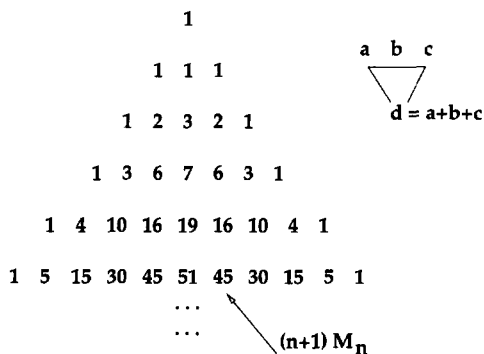


Fig. 21.

(I) With an equation of the form  $y = 1 + xf(y)$ , for  $y = \sum a_n x^n$  and  $a_0 = 1$ , let  $D = d/dt$ . Then

$$a_n = \frac{1}{n!} [D^{n-1} f^n(t)]_{t=1}.$$

(II) With an equation of the form  $z = xf(z)$ , for  $z = \sum_{n \geq 1} a_n x^n$ ,

$na_n$  is the coefficient of  $t_{n-1}$  in  $(f(t))^n$ .

Passage from (I) to (II) is usually by  $z = xy$  or a similar transformation. The Catalan equation  $y = 1 + xy^2$  is in the form demanded by (I), and thus

$$n!C_n = D^{n-1} [t^{2n}]_{t=1} = (2n)(2n-1) \cdots (n+2) = \frac{(2n)!}{(n+1)!}.$$

Alternately, with  $z = xy$  we have

$$y = 1 + xy^2, \quad xy = x + (xy)^2, \quad z = x + z^2,$$

$$z - z^2 = x, \quad z = \frac{x}{1-z}.$$

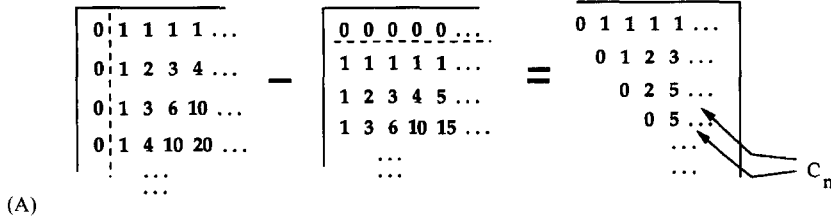
Consequently,  $(n+1)C_n$  is the coefficient of  $t^n$  in  $(1-t)^{-(n+1)}$ , namely  $\binom{2n}{n}$ .

The Motzkin equation  $y = 1 + xy + (xy)^2$  is the same as  $\frac{z}{x} = 1 + z + z^2$  and so  $(n+1)M_n$  is the coefficient of  $t^n$  in  $(1+t+t^2)^{n+1}$ . The powers of  $1+t+t^2$  are easily computed in a Pascal-like triangle (see Fig. 21). Each number is the sum of three above it. For example,  $7 + 6 + 3 = 16$ . The central numbers were mentioned in the last section.

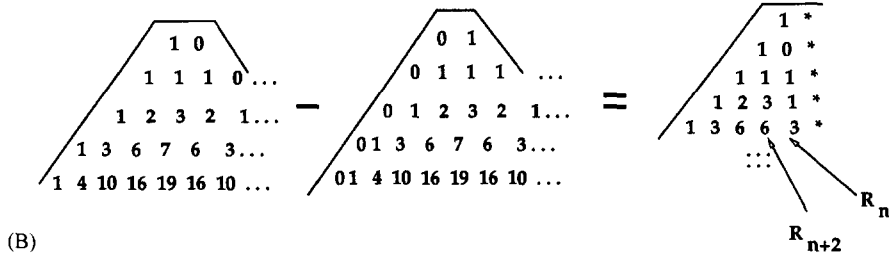
If the power is written  $((1+t) + t^2)^{n+1}$ , two applications of the binomial expansion lead to

$$(n+1)M_n = \sum_{i=0} \binom{n+1}{i} \binom{n+1-i}{i+1} = \sum_i \frac{(n+1)!}{i!(i+1)!(n-2i)!}.$$

**SUPERIMPOSE PASCAL RECTANGLES TO GET CATALAN TABLE**



**SUPERIMPOSE TRINOMIAL TABLES TO GET A RIORDAN TRIANGLE**



**A DIFFERENT COMBINATION GETS A MOTZKIN TRIANGLE**

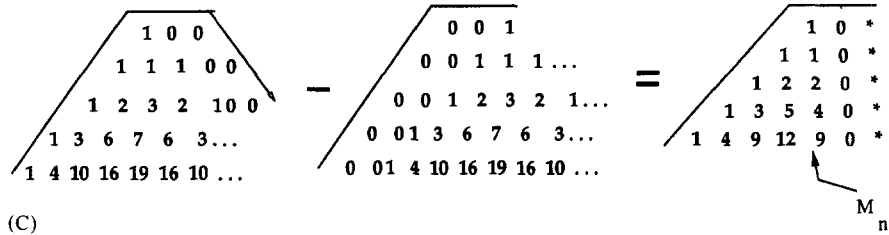


Fig. 22.

The equation for the Riordan enumerator,  $y = \frac{1}{1+x} + xy^2$  becomes  $z = \frac{x}{1+x} + z^2$ , or  $z = x(\frac{1}{1-z} - z)$ . Here the factor  $\frac{1}{1-z} = 1 + xM(x)$  gives  $z = xR(x)$ . Thence,  $(n + 1)R_n$  is the coefficient of  $t^n$  in  $(\frac{1}{1-t} - t)^{n+1}$ , which, by two applications of the binomial expansion, gives

$$(n + 1)R_n = \sum_{i=0}^n (-1)^i \binom{n + 1}{i} \binom{2n - 2i}{n - i}.$$

Earlier we observed a Catalan family determined by the restricted motion of a chess king on an infinite triangular chessboard. The simple recursion that counts how many ways it can get to a given square is reproduced by shifting the Pascal triangle (in rectangle presentation) and subtracting it from itself (see Fig. 22A and [36]). Here the negative numbers are not shown. The diagonal above the zeroes is

$$C_n = \binom{2n}{n} - \binom{2n}{n - 1} = \frac{1}{n + 1} \binom{2n}{n}.$$

The same trick applied to the trinomial coefficients gives Motzkin and Riordan number triangles (Fig. 22B and Fig. 22C).

## 7. Extras and leftovers

We finish off our survey by briefly describing connections with the theory of chromatic polynomials (the common abbreviation ‘chromials’ will be used). A fuller treatment is planned. Basic information on chromials can be found in Biggs [8], Read [29], Read and Tutte [30].

Briefly, if  $G$  is a finite graph without loops, and the set of colors is  $\{1, 2, \dots, \lambda\}$ , then there is a polynomial  $P = P(G, \lambda)$  which counts the number of colorings of the graph with  $\lambda$  colors: a coloring being a mapping of vertices to colors which never uses the same color on the ends of an edge.

Two modifications will be needed: (a) some vertices can have fixed colors pre-assigned, and (b) some edges may be designated as ‘contractive’. Contractive edges require the same color at both ends; thus coloring such a graph is essentially the same as contracting the contractive edges first, and then coloring the graph. In making some edges contractive, we must be careful that no loops arise when the contraction is performed. Note that multiple edges are a harmless nuisance, and can be suppressed.

The original motivation for studying chromials of planar graphs was the hope of approaching the Four Color Problem by quantization, analysis, and then specialization (put  $\lambda = 4$ ).

For many years the bible for the theory of chromials of maps and graphs was the 1946 monograph ‘Chromatic Polynomials’ of Birkhoff and Lewis [10], hereafter denoted CP. These authors paid much attention to maps  $M$  defined by a trivalent (or *cubic*) plane graph, and a ring of  $n$  regions in such a graph. Once a ring is selected, the map may be ‘reduced’ by ‘deleting’ one side of the ring. Topologically, a ‘proper’ ring is an annulus, separating two topological disks. To reduce the map, you contract one of the disks to a point.

It is often convenient to dualize (see Fig. 23). The trivalent map  $M$  is replaced with a plane graph  $G$  whose regions are triangles. Two vertices of  $G$  joined by an edge replace two regions sharing a common boundary. A ‘ring’ is then a simple circuit  $R$  in  $G$ , called proper if it has at least one vertex on each side, and no chord edges (edges connecting nonconsecutive vertices of  $R$ ). The chromial of  $M$  is then identical to the chromial of  $G$ .

Reduction is simple: just delete all vertices and edges on one side of  $R$ . The reduced graph  $H$  can now be represented as a plane near-triangulation, or PNT, with perimeter  $R$ . That is,  $R$  is a convex plane polygon, with only one exterior face, and all interior faces are triangles. A ‘degenerate’ reduction may further modify the exterior face: ring vertices which are nonadjacent can be joined by an edge or even coalesced. This may be done by putting regular and/or contractive edges in the exterior face in a noncrossing way. Note: the ring ceases to be a proper ring.



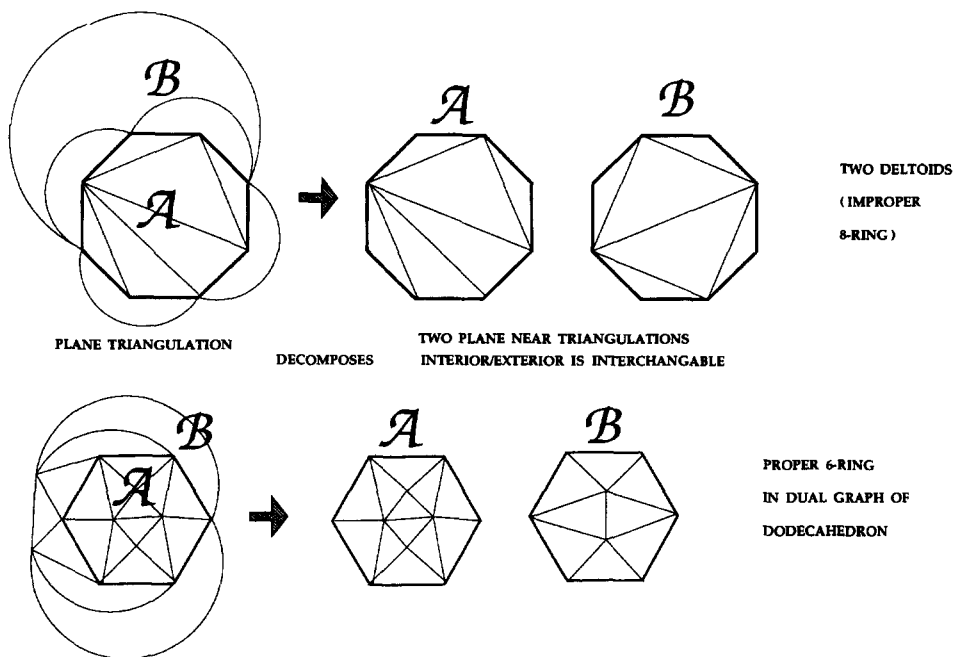


Fig. 23.

One may use these ‘degenerate’ reductions to create smaller cubic maps (dually, smaller planar triangulations) from a given one. A chief goal in the paper CP is to reconstruct the ‘chromial’ of the entire map by combining in some fashion chromials associated with the reduced maps for a fixed ring  $R$ . (The reduced maps were called ‘free’, so the chromials were called ‘free’ chromials. Here the term *F-chromial* will be used.) Success in the reconstruction was achieved only after a new kind of chromial was introduced.

Consider PNT graph  $H$  with a labeled boundary circuit  $R$ . We assume the labeling proceeds counterclockwise from the bottommost edge in the diagram. This labeling is implicit, so that 1, 2, 3, ... may be used for colors.

A coloring of ring  $R$  alone is a pre-coloring of  $H$ . We recall the definition of the scheme of a partition. Each feasible partition of the ring vertices may be represented by an orthodox color scheme. The eleven orthodox schemes for a 5-ring are

With crossings : 12123, 12132, 12134, 12312, 12313,

Noncrossing : 12314, 12323, 12324, 12342, 12343, 12345.

Arbitrary schemes can be ‘converted’ by permutation of colors to orthodox equivalents, for example, 232141 converts to 121343.

We know that the orthodox schemes of length  $n$  form a set with  $V_n$  members. Following CP, we precolor the ring using a selected scheme  $\sigma$ , and then find a chromial  $P_\sigma = P(H^\sigma, \lambda)$  for the precolored graph  $H^\sigma$ . Equivalent schemes lead to the

same chromial, which is the reason that only orthodox schemes are needed. Thus a set of chromials, the so-called ‘constrained chromials’ is obtained, and there are  $V_n$  members.

By means of C-chromials, CP found a simple way to reconstruct the desired chromial. But they were not satisfied, because they wanted F-chromials.

In brief, an F-chromial for graph  $G$  is found by replacing one of the two NPT graphs with common boundary  $R$  by an elementary degenerate sort of NPT (specified and enumerated below), and evaluating the chromial. We introduce  $A_n$  as the number of such chromials using just one NPT  $H$ .

From our point of view, both C-chromials and F-chromials are constrained, only in different ways. Now it happens (for fixed  $H$ ) that each F-chromial is a sum of certain slightly modified C-chromials. Assuming an inverse solution (each C-chromial is a linear combination of F-chromials), then the goal of CP has been achieved — the chromial for  $G$  is initially given as a combination of C-chromials, but may be reexpressed in terms of F-chromials. Thus the chromial for  $G$  is reconstructed from chromials of smaller triangulation graphs.

For fixed PNT graph  $H$ , we may stipulate that the  $V_n$  distinct C-chromials are enumerated  $p_1, p_2, p_3, \dots$  and that the  $A_n$  distinct F-chromials are enumerated  $q_1, q_2, q_3, \dots$ . Certain curious facts are now noted. Each group of chromials (C- or F-) is subject to a variety of linear identities that are independent of the choice of  $H$ . In CP the C-chromials identities are much studied, but the F-identities are given little attention. However, the latter may be recovered using their ‘twisting the boundary’ formula (we will return to this shortly).

The C-identities, on the other hand, were more elusive. They were obtained in CP apparently by trial and error, and only for the lowest orders  $n = 4, 5$ . An extension to  $n = 6$  was done later by Hall and Lewis [24]. Even with all their computation, the general form and provenance of these identities remained somewhat mysterious, but once obtained, CP was able to employ them to invert the F-to-C connection, and thence to complete the reduction program.

The mystery remained for some 30 years. In the meanwhile, my father, Arthur Bernhart, made adaptations in case  $\lambda = 4$ , obtaining numerous equations involving ‘frequencies’. These frequencies were essentially C-chromial values at  $\lambda = 4$ , but only using schemes with four colors or less. The equations were obtained by direct appeal to Kempe chains [5].

In the mid-1970s, while I was a visitor at the University of Waterloo, W. T. Tutte introduced a useful distinction: ring color schemes were called planar if the associated (feasible) partition was noncrossing, and similarly, C-chromials obtained from a planar coloring scheme were planar [46]. He then recast the known C-identities, and demonstrated that they were just sufficient to express nonplanar C-chromials in terms of planar ones. In this form, the identities are now known as *flattening equations*. For my part, I found a method of generating the identity which ‘flattens’ any given non-planar C-chromial, and was able to count these identities by finding the key recurrence for the feasible NC partitions. A joint paper is planned.

We now return to the F-chromial set. In hindsight, a careful study of the F-identities would have been very useful, because it is not difficult to construct a basis of independent F-chromials. This basis sheds light on the corresponding ‘planar’ basis for C-chromials. It is logical to consider the common basis size  $R_n$  to be the ‘linear dimension’ of the ring of length  $n$ .

We now digress to consider the nature of the degenerate PNT in the definition of an F-chromial. Start with a convex  $n$ -gon, representing the ring  $R$ . The imprecise notion of filling the interior with contractive and regular diagonals can be made clearer by using a deltoid as a seed, and a color scheme as a catalyst. In diagrams, the contractive diagonals will be distinguished by doubling, so that they resemble the double bonds of chemistry.

More precisely, we let  $T^\sigma$  be a deltoid (member of [C1]) precolored with scheme  $\sigma$ . There are  $C_n \cdot V_n$  of these. Then we examine the  $n - 3$  inner edges, changing the edges to double bonds just in case the ends are the same color. This makes the precoloring a valid coloring. An elementary configuration results when we discard the coloring, and (optionally) contract all double bonds (see Fig. 24A).

Varying the initial deltoid, or the precoloring, does not necessarily change the outcome. Without going into the details, it is convenient for diagrams to leave the double bonds uncontracted, but to remove certain ‘redundant’ diagonals. For example, if the graph contains a circuit with edges  $x, y$  of like type, and all circuit edges other than these two are double bonds, then one of  $x, y$  may be omitted without loss. It is also no loss to require that the double bonds follow the rules laid down above for the graph of a partition. Each class of the partition is, of course, a group of vertices which are merged if the contraction is performed.

No matter which deltoid  $D$  is used as ‘seed’, some color schemes will produce no double bonds. Thus, all the deltoids (for an  $n$ -gon) qualify as elementary configurations. For  $n = 4$  we have a square  $abcd$  with one diagonal (either  $ac$  or  $bd$  which may be either contractive or not. Hence  $A_4 = 4$ . For  $n = 5$ , in addition to  $C_3 = 5$  deltoids, a sole contractive diagonal may be inserted in five ways; thus  $A_5 = 10$  (see Fig. 24B).

These graphs were called ‘options’ or ‘constraints’ for many years by Arthur Bernhart [4], who was able to compute the sequence  $A_n$  by a complex recursion (private notes and conversation). We will think of them as Arthur’s constraints, or briefly: *arkons*. The sequence  $A_n$  is M3400 in [42]. For  $n = 2, \dots, 13$  we have

$$1 \quad 1 \quad 4 \quad 10 \quad 34 \quad 112 \quad 398 \quad 1443 \quad 5387 \quad 20482 \quad 79177 \quad 310102.$$

The ‘outline’ of an arkon is formed by omitting the noncontractive diagonals. An outline may be considered a feasible partition. Take the graph of the partition, double all the edges, and add the surrounding polygon  $R$  made of regular edges. This is a simple variation of the class [R2]. When the double bonds are contracted, a tree-like *cactus* is obtained. A standard tree is made of edges; a cactus is made of circuits (or ‘cells’).

Conversely, one obtains an arkon from a cactus by putting a deltoid in each cell. If a *bramble* is a cactus in which each cell has at most three sides, there is nothing to be

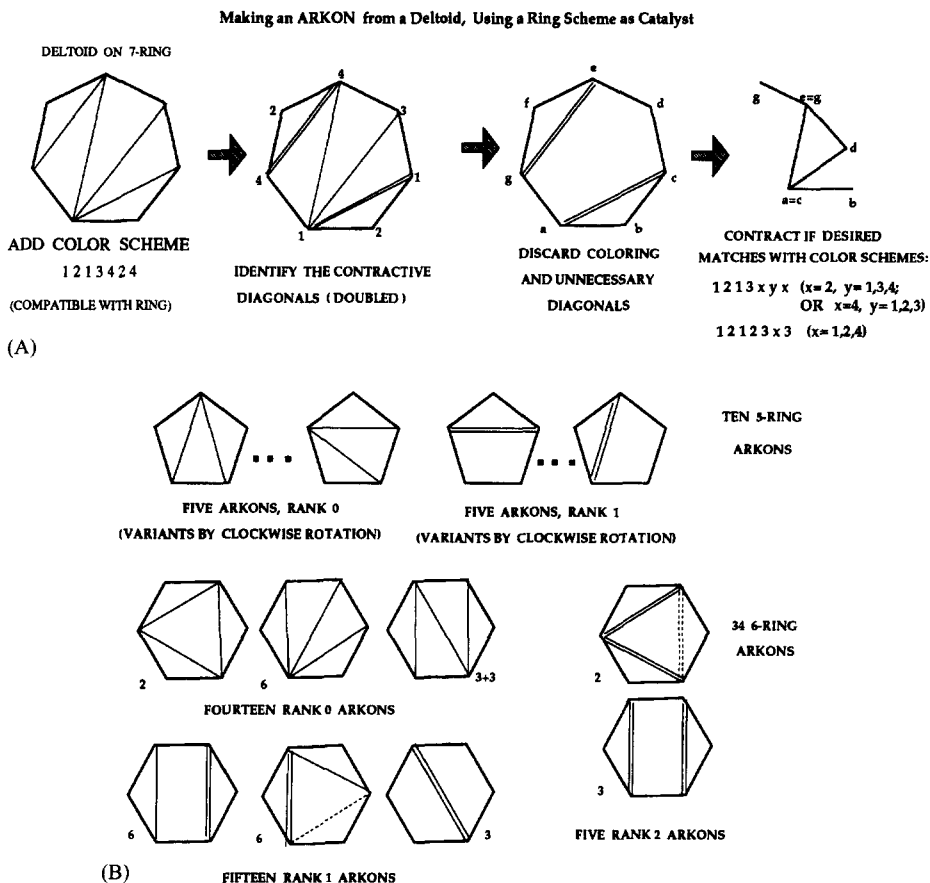


Fig. 24.

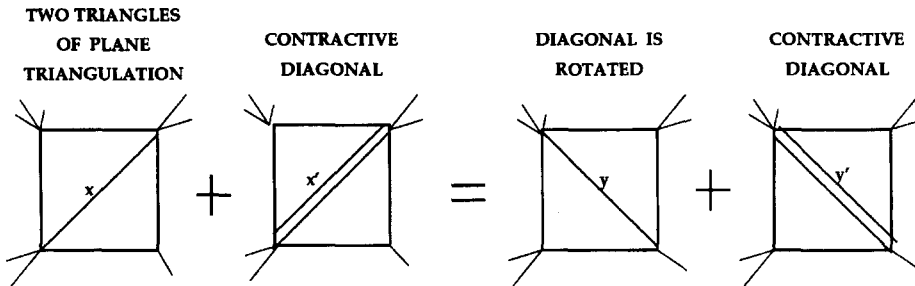
done — we can regard the brambles as the intersection of the cactii and the arkon. We will call two arkon *related* if they have the same outline (can be built out of the same cactus).

Let the *rank* of an arkon be the number of cells in the outline. Hence an arkon of lowest rank is just a deltoid, and vice versa. An arkon of highest rank is a bramble with at most one 3-sided cell.

Let  $q_i, q_j$  be two F-chromials, obtained from related arkon (having the same outline). Our immediate goal is to show as a corollary to the ‘twisting the boundary’ equations of CP, that there is a linear identity of the form  $q_i + \dots = q_j + \dots$ , where all chromials other than  $q_i, q_j$  have higher rank.

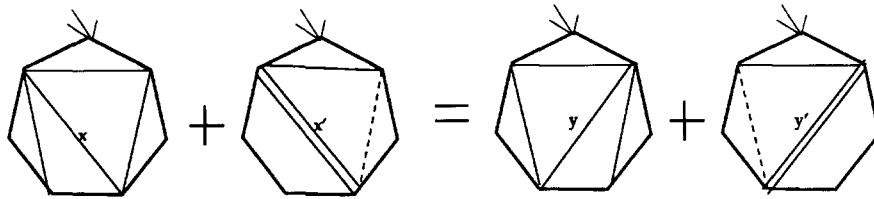
First we restate the CP equations in our format. Let  $H$  be a PNT of order four, and consider the arkon  $E_1, E_2, E_3, E_4$  of order four. If each one is combined by ring identification with  $H$ , four reduced ‘free’ graphs are obtained (see Fig. 25 (top)). In this equation, following a common convention, each graph diagram stands for its chromial.

**BIRKHOFF - LEWIS TWISTING THE BOUNDARY EQUATION  
EACH DIAGRAM STANDS FOR A WHOLE MAP CHROMIAL**



**4-RING INTERPRETATION: THE 4 ARKONS (INSIDE THE SQUARE)  
ARE COMBINED WITH ARBITRARY FIXED EXTERIOR (NPT)**

**N-RING INTERPRETATION, N>4: THE SQUARE REPRESENTS TWO  
ADJOINING TRIANGLES OF SOME ARKON (JOINED TO NPT)  
IF 1ST,3RD ARKONS HAVE RANK k, THEN 2ND,4TH HAVE RANK k+1**



**7-RING INTERPRETATION OF EQUATION  
CHANGES OCCUR IN 4-GON WITH DIAGONAL x  
DOTTED DIAGONALS MAY BE OMITTED AS WELL**

Fig. 25.

The equation is nearly trivial, for either sum is just the chromial of  $H$ : the first graph captures the colorings with the ends of the diagonal colored distinctly, and the second graph captures the colorings with the ends of the diagonal colored the same.

We now reinterpret the squares of the first diagram as a pair of adjoining triangles in some arkon of order  $n > 4$ . An appropriate  $H$  is joined with it. The remaining three terms of the equation are similarly reinterpreted. In Fig. 25 (bottom) we choose for illustration a deltoid arkon with a seven-sided boundary. The square is composed of the triangles which share the diagonal edge marked  $x$ . The reinterpreted equation involves four arkons that have ranks 1, 2, 1, 2.

More generally, we can find a similar four term identity ('quartet') in which the four arkons, say  $E_i, E_j, E_m, E_n$ , are such that  $E_i, E_m$  differ by twisting the edge  $x$ , and so have the same rank. The other two have the next highest rank. But, if two arkons have the same outline, it is easy to see that twisting edges can change one to the other in a

finite number of steps. Each step yields a quartet equation, and chaining the equation proves the corollary.

It now follows that for an F-chromial basis, we need only take one arkon with any given cactus as outline, and  $R_n$  is the dimension. In CP this number is called  $v(n)$ , and calculated only for the smallest cases.

The authors of CP shy away from working with maps that are not defined by cubic graphs. Put dually, they restrict their elementary configurations to arkons. But think of how much better it is to use cacti (outlines) to define the F-chromials. Thus a reduced graph is obtained by erasing one side of the ring circuit, and then picking any feasible NC partition of vertices, and finally merging the vertices of each class. A planar graph results, but each large cell is a large non-triangular face.

Counting arkons, brambles, and similar classes by means of Lagrange inversion is eminently feasible, but too much for inclusion in this article. Details will be given elsewhere. The number  $A_{n,k}$  of arkons of order  $n$  and rank  $k$  is

$$\frac{1}{n-k-1} \binom{n}{k} \binom{2n-3k-4}{n-2k-2}$$

and, of course,  $A_n = A_{n,0} + A_{n,1} + \cdots + A_{n, \lfloor \frac{n}{2} \rfloor - 1}$ . The presence of the simple factor  $\binom{n}{k}$  is intriguing; is there a direct combinatorial justification for this formula?

In my dissertation (1974) I used  $K_n$  in place of  $A_n$ , and exhibited a certain recursion. Rediscovery of the ring numbers  $R_n$  led to a Catalan-like recursion a few years later. I had not encountered  $M_n$  or the companion sequence. Checking [41] did not help, and [42] did not exist. I am indebted to correspondence with D. G. Rogers for the  $R$ – $M$  connection and pointing me toward the effective enumeration of  $R_n$  and  $A_n$  by Lagrange Inversion.

Over the course of two decades, my view of the sequences  $C_n, M_n$  and  $R_n$  as a close-knit family took shape. The most concrete visualization of this is perhaps the pair of difference triangles of Section 4. It is now well known that the Catalan numbers enumerate an amazing variety of interesting classes. I hope that it has been shown in this paper that Motzkin and Ring numbers are not far behind. In any case, I have sought to create a primer on the three sequences, and also many of the commoner tools of combinatorics.

## References

- [1] G. Almkvist, W. Dicks, E. Formanek, Hilbert series of fixed free algebras and noncommutative classical invariant theory, *J. Algebra* 93 (1) (1985) 189–214.
- [2] D.L. Andrews, T. Thirunamachandran, On three-dimensional rotational averages, *J. Chem. Phys.* 67 (11) (1977) 5026–5033.
- [3] E. Barucci, R. Pinzani, R. Sprugnoli, The Motzkin family, *Pure Math. Appl. Ser. A* 2 (3–4) (1991) 249–279.
- [4] A. Bernhart, Six rings in minimal five color maps, *Amer. J. Math.* 69 (1947) 391–412.
- [5] A. Bernhart, Chromatic equations, in: Bondy, Murty (Eds.), *Graph Theory and Related Topics*, Academic Press, New York, 1979.

- [6] F. Bernhart, P.C. Kainen, The book thickness of a graph, *J. Combin. Theory Ser. B* 27 (1979) 320–331.
- [7] F. Bernhart, Some classes of N-ring graphs, in preparation.
- [8] N. Biggs, *Algebraic Graph Theory*, 2nd ed., Cambridge University Press, Cambridge, 1993.
- [9] G.D. Birkhoff, The reducibility of maps, *Amer. J. Math.* 35 (1913) 115–128.
- [10] G.D. Birkhoff, D.C. Lewis, Chromatic polynomials, *Trans. Amer. Math. Soc.* 60 (1946) 341–355.
- [11] W.G. Brown, Historical note on a recurrent combinatorial problem, *Amer. Math. Monthly* 72 (9) (1965) 973–977.
- [12] R. Chapman, Moments of Dyck paths, *Discrete Math.* 204 (this Vol.) (1999) 113–117.
- [13] F.R.K. Chung, F.T. Leighton, A.L. Rosenberg, Embedding graphs in books: a layout problem with applications to VLSI design, *SIAM J. Algebra Discrete Meth.* 8 (1) (1987) 33–58.
- [14] J.H. Conway, H.S.M. Coxeter, Triangulated polygons and frieze patterns, *Math. Gazette* 57 (1973) 87–94, 175–183.
- [15] N.G. de Bruijn, B.J.M. Morselt, A note on plane trees, *J. Combin. Theory Ser. 2* (1967) 27–34.
- [16] E. Deutsch, Dyck path enumeration, *Discrete Math.* 204 (this Vol.) (1999) 167–202.
- [17] C. Domb, A.J. Barrett, Enumeration of ladder graphs, *Discrete Math.* 9 (1974) 341–358.
- [18] R. Donaghey, Restricted plane tree representations of four Motzkin–Catalan equations, *J. Combin. Theory (A)* 22 (1977) 114–121.
- [19] R. Donaghey, Automorphisms on Catalan trees and bracketings, *J. Combin. Theory (B)* 29 (1980) 75–90.
- [20] R. Donaghey, L.W. Shapiro, Motzkin numbers, *J. Combin. Theory (A)* 23 (3) (1977) 291–301.
- [21] A. Errera, Un problème d'énumération, *Mém. Acad. Royale Bruxelles 8°* (2) 11 (6) (1931).
- [22] H.W. Gould, *Research Bibliography of Two Special Sequences*, Rev. ed., Combin. Research Institute, Morgantown, West Virginia, 1977.
- [23] I.P. Goulden, D.M. Jackson, *Combinatorial Enumeration*, Wiley, New York, 1983.
- [24] D.W. Hall, D.C. Lewis, Coloring six-rings, *Trans. Amer. Math. Soc.* 64 (1948) 184–191.
- [25] Ph. Hanlon, Counting interval graphs, *Trans. Amer. Math. Soc.* 272 (2) (1982) 383–426.
- [26] St.J.G. Kettle, A class of natural bijections between Catalan families, in: E.J. Billington, Sh. Oates-Williams, A.P. Street (Eds.), *Combinatorial Mathematics*, Proc. 9th Australian Conf. on Combin. Math., Univ. Queensland, Brisbane, Australia, Aug. 24–28, 1981, *Lecture Notes in Math.*, Vol. 952, Springer, Berlin, 1982, pp. 327–348.
- [27] T. Motzkin, Relations between hypersurface cross ratios, and a combinatorial formula for partitions of a polygon, for permanent preponderance, and for nonassociative products, *Bull. Amer. Math. Soc.* 54 (1948) 352–360.
- [28] H. Prodinger, A correspondence between ordered trees and noncrossing partitions, *Discrete Math.* 46 (1983) 205–206.
- [29] R.C. Read, An introduction to chromatic polynomials, *J. Combin. Theory* 4 (1968) 52–71.
- [30] R.C. Read, W.T. Tutte, Chromatic polynomials, in: L.W. Beineke, R.J. Wilson (Eds.), *Selected Topics in Graph Theory*, vol. 3, Academic Press, London, 1988, pp. 15–42.
- [31] J. Riordan, Enumeration of plane trees by branches and endpoints, *J. Combin. Theory (A)* 19 (1975) 214–222.
- [32] D.G. Rogers, Similarity relations on finite ordered sets, *J. Combin. Theory Ser. A* 23 (1977) 88–98.
- [33] D.G. Rogers, The enumeration of a family of ladder graphs, Part I: connective relations, *Quart. J. Math. Oxford* 28 (1977) 421–431.
- [34] D.G. Rogers, The enumeration of a family of ladder graphs, Part II: Schröder and superconnective relations, *Quart. J. Math. Oxford* 31 (1980) 491–506.
- [35] D.G. Rogers, Rhyming schemes: crossings and coverings, *Discrete Math.* 33 (1981) 67–77.
- [36] L.W. Shapiro, A Catalan triangle, *Discrete Math.* 14 (1976) 83–90.
- [37] L.W. Shapiro, A short proof of an identity of Touchard's concerning Catalan numbers, *J. Combin. Theory Ser. A* 20 (1976) 375–376.
- [38] L.W. Shapiro, Positive definite matrices and Catalan numbers, revisited, *Proc. Amer. Math. Soc.* 90 (3) (1984) 488–496.
- [39] R. Simion, D. Ullman, On the structure of the lattice of noncrossing partitions, *Discrete Math.* 98 (1991) 193–206.
- [40] D. Singmaster, An elementary evaluation of the Catalan numbers, *Amer. Math. Monthly* 85 (1978) 366–368.
- [41] N.J.A. Sloane, *A Handbook of Integer Sequences*, Academic Press, San Diego, 1973.

- [42] N.J.A. Sloane, S. Plouffe, *The Encyclopedia of Integer Sequences*, Academic Press, San Diego, 1995.
- [43] W.T. Tutte, A contribution to the theory of chromatic polynomials, *Canad. J. Math.* 6 (1954) 80–91.
- [44] W.T. Tutte, Chromials, in: C. Berge, D. Ray-Chaudhuri (Eds.), *Hypergraph Seminar*, Ohio State University, 1972, *Lecture Notes in Mathematics*, vol. 411, Springer, Berlin, 1974, pp. 243–266.
- [45] W.T. Tutte, On the Birkhoff–Lewis equations, *Discrete Math.* 92 (1991) 417–425.
- [46] W.T. Tutte, Chromials, in: D.R. Fulkerson (Ed.), *Studies in Graph Theory, Part II*, *MAA Studies in Mathematics*, vol. 12, The Mathematical Association of America, 1975, pp. 361–377.
- [47] H.S. Wilf, *generatingfunctionology*, 2nd ed., Academic Press, New York, 1994.